Table of Contents

Program at a Glance

Time	Topic and Speakers
Sunday, October 23	
2:00– 5:30 pm	**Pre-meeting Radiobiology Seminar**
2:00–3:00 pm	**Radiobiology Session** I (*Session Chairs: Piero Fossati, MD, and John Eley, PhD)*
3:00–3:40 pm	**Break**
3:40–5:30 pm	**Radiobiology Session II** (*Session Chairs: Piero Fossati, MD, and John Eley, PhD)*
6:30–9:00 pm	**Memphis Blues at the Beale Street Landing (*hors d'oeuvres*)** (*Sponsored by RaySearch*)
Monday, October 24	
7:30–8:40 am	**Sunrise Session 1: Adult**
8:45–9:00 am	**Welcome and Opening Remarks**
9:00–9:30 am	**Emerging Indications Session** (*Session Chairs: Hesham Gayar, MD, and James Metz, MD)*
9:30–10:10 am	**The Cutting Edge Session: Adaptive Particle Therapy** (*Session Chairs: Nancy Mendenhall, MD, and Jeffrey Bradley, MD)*
10:10–10:40 am	**Break**
10:40–11:40 pm	**Original Contributions Session I** (*Session Chairs: Marcio Fagundes, MD, and Andrew Lee, MD)*
11:40 am–1:00 pm	**Lunch** (*Sponsored by Varian; Domino's Event Center*)
1:00–2:00 pm	**Original Contributions Session II** (*Session Chairs: Carl Rossi Jr., MD, and Brian Chon, MD)*
2:00–3:30 pm	**Poster Session and Break** (*Session Chairs: David Followill, PhD, and Jonathan Ashman, MD*)
3:30–4:30 pm	**General Assembly**
6:30–9:00 pm	**Dinner at the National Civil Rights Museum** (*Sponsored by Mevion*)
Tuesday, October 25	
7:30–8:45 am	**Sunrise Session 2: Lung**
9:00–9:50 am	**Clinical Trials Update Session I** (*Session Chairs: Nancy Mendenhall, MD, and Alex Lin, MD)*
9:50–10:30 am	**Break**
10:30–11:20 am	**Clinical Trials Update Session II (***Session Chairs: Steven Frank, MD, and William Hartsell, MD)*
11:20 am–12:30 pm	**Lunch** (*Sponsored by IBA; Domino's Event Center*)
12:30–1:30 pm	**Keynote: Why Do We Need Carbon Ions?** *Introduction: Eugen Hug, MD; Speaker: Marco Durante, PhD*
1:30–2:30 pm	**Original Contributions Session III** (*Session Chairs: Bradford Hoppe, MD, MPH, and Oren Cahlon, MD)*
2:30–3:20 pm	**Poster Session and Break**
3:20–4:10 pm	**Pediatric Session I** (*Session Chairs: Torrun Yock, MD, and Daniel Indelicato, MD)*
4:15–5:15 pm	**Is Proton Therapy the Ideal Tool for Hypofractionation?**
6:30–9:00 pm	**Gala at the Bass Pro Shop at the Memphis Pyramid** (*Sponsored by Hitachi*)
Wednesday, October 26	
7:30–8:45 am	**Sunrise Session 3: Pediatric**
9:00–10:00 am	**Pediatric Session II** (*Session Chairs: Anita Mahajan, MD, and Andrew Chang, MD)*
10:00–10:30 am	**Break**
10:30–11:30 am	**Physics Session** (*Session Chairs: Narayan Sahoo, PhD, and Mark Pankuch, PhD, DABR)*
11:30 am–11:45 am	**Closing Remarks**

Welcome Letter

October 23, 2016

On the behalf of the Particle Therapy Co-Operative Group North-America (PTCOG-NA) and the 2016 annual conference organizing committee, we welcome you to the 3rd Annual PTCOG-NA Conference. The theme for this conference is Advancing Particle Therapy: Challenge and Innovation in Adult and Pediatric Oncology, and we anticipate that you will find numerous opportunities to gain new knowledge, share technical and clinical experiences, network with colleagues, and communicate with industry partners.

The conference will focus on advances in IMPT, robustness in treatment planning, quantifying and managing the uncertainty in range and tumor motion, incorporating 3-D imaging with daily delivery, and biological effects. The clinical applications will center on the traditionally recognized clinical indications but more importantly on pediatric cancers, and cancers of the breast, lung, head and neck, and gastrointestinal tract. Hypofractionation and combined modality approaches will also be an important focus. We anticipate updates on clinical trials, and lively discussions around future protocols, grant opportunities, and multi-institutional collaborative efforts, as well as recognizing the value of large multi-center registry data.

In addition to attending the conference, we invite you to experience the Bluff City, Memphis, Tennessee, on the banks of the Mississippi River offering an expansive variety of things to see and do. This city offers attractions for guests of all ages and from around the world. Memphis is known for its music and food. Blues, jazz and rock 'n' roll spill out from the clubs along Beale Street, and restaurants dish up barbecue and soul food. Elvis Presley, B.B. King and Johnny Cash recorded albums at the legendary Sun Studio, and Presley’s Graceland mansion is a popular attraction.

This Annual PTCOG-NA Conference will enhance your knowledge of adult and pediatric oncology, widen your network, and expand your outlook while providing a relaxing and memorable time in our beautiful city. We are very excited about this event and welcome you to Memphis.

Sincerely,

Eugen B. Hug, MD, President
Hesham E. Gayar, MD, Vice President
Anita Mahajan, MD, Secretary
Carl Rossi, Jr., MD, Treasurer
Jonathan B. Farr, DSc, Local Conference Host

Conference Planning Committee

Jonathan B. Farr, DSc
Chief, Radiation Physics
Department of Radiation Oncology
St. Jude Children's Research Hospital
Memphis, TN

Hesham E. Gayar, MD
Department of Radiation Oncology
Karmanos Cancer Institute
Flint, MI

William F. Hartsell, MD
Medical Director
Northwestern Medicine Chicago Proton Center
Warrenville, IL

Eugen B. Hug, MD
International Program Director
Procure Proton Therapy Center
Somerset, NJ
Medical Director
MedAustron Ion Therapy Center,
Wiener Neustadt, Austria

Anita Mahajan, MD
Professor, Department of Radiation Oncology
The University of Texas MD Anderson Center
Houston, TX

Carl Rossi, Jr., MD
Medical Director
Scripps Proton Therapy Center
San Diego, CA

Conference Information

Conference Venues

The scientific and educational sessions will be held in the Auditorium of the Marlo Thomas Center (MTC) for Global Education and Collaboration at St. Jude; breaks, exhibits, and posters can be found in the MTC Atrium outside the Auditorium (see a map of the MTC at the end of this program book). The MTC sits atop the world's first proton therapy center designed for and dedicated solely to the treatment of children.

Sponsored lunches on Monday and Tuesday will be held in the Domino's Event Center (see building OE on the St. Jude campus map at the end of this program book). The Event Center, which opened in August 2015, is in a 1911 building that originally housed the Memphis Artesian Water Department and retains many original features, combined with modern additions.

Evening social events will be held at Memphis landmarks such as Beale Street Landing, the National Civil Rights Museum, and Bass Pro Shop at the Memphis Pyramid.

Educational Information

After attending this educational conference, you should be able to:

- Describe the principles behind proton therapy and its effective use in the treatment of cancer
- Evaluate new techniques and systems for proton therapy

This activity has been planned and implemented in accordance with the accreditation requirements and policies of the Accreditation Council for Continuing Medical Education (ACCME) through the joint providership of St. Jude Children's Research Hospital and the Particle Therapy Cooperative Group-North America. St. Jude Children's Research Hospital is accredited by the ACCME to provide continuing medical education for physicians.

The educational content of this conference was developed without commercial support.

For more information about financial disclosures of planners, speakers, and other individuals in control of content as well as completing the evaluation for this conference and claiming CME credit, please see the CME insert.

Conference Endorsements and Exhibitors

Endorsements

AAPM is a scientific and professional organization, founded in 1958, composed of more than 8000 scientists whose clinical practice is dedicated to ensuring accuracy, safety and quality in the use of radiation in medical procedures such as medical imaging and radiation therapy. They are generally known as medical physicists and are uniquely positioned across medical specialties due to our responsibility to connect the physician to the patient through the use of radiation producing technology in both diagnosing and treating people. The responsibility of the medical physicist is to assure that the radiation prescribed in imaging and radiation therapy is delivered accurately and safely.

One of the primary goals of AAPM is the identification and implementation of improvements in patient safety for the medical use of radiation in imaging and radiation therapy.

ASTRO is the premier radiation oncology society in the world, with more than 10,000 members who are physicians, nurses, biologists, physicists, radiation therapists, dosimetrists and other health care professionals who specialize in treating patients with radiation therapies. These medical professionals, found at hospitals, cancer treatment centers and academic research facilities around the globe, make up the radiation therapy treatment teams that are critical in the fight against cancer. Together, these teams, treat more than 1 million cancer patients each year. As the leading organization in radiation oncology, the Society is dedicated to improving patient care through professional education and training, support for clinical practice and health policy standards, advancement of science and research and advocacy.

Exhibitors

Please stop by our exhibitor tables during your break. Our exhibitors include:

- Hitachi (Diamond)
- Mevion Medical Systems (Platinum)
- RaySearch (Gold)
- Varian Medical Systems (Gold)
- IBA Proton Therapy (Gold)
- Orfit Industries (Silver)
- ProTom International (Silver)
- .decimal (Silver)

Agenda

Time	Topic and Speakers
Sunday, October 23	
2:00– 5:30 pm	**Pre-meeting Radiobiology Seminar**
2:00 – 3:00pm	**Radiobiology Session I** *Session Chairs: Piero Fossati, MD, CNAO, and John Eley, PhD, University of Maryland*
2:00 pm	Radiobiology and Physics of Particle Microbeams *John Eley, PhD, University of Maryland*
2:50 pm	The Dose-Weighted LET and Relative Biological Effectiveness (RBE) for DNA Double Strand Break (DSB) Induction for IMPT with Spot Scanning Pencil Beam and for Conventional Technique Using Broad Proton Beams with Patient-Specific Aperture and Compensator *Vadim Moskvin, PhD, St. Jude Children's Research Hospital*
3:00 pm	Break
3:40–5:30 pm	**Radiobiology Session II** *Session Chairs: Piero Fossati, MD, CNAO, and John Eley, PhD, University of Maryland*
3:40 pm	Pre-Clinical Study of the Effects of Duocarmycin SA and Proton Radiation on Glioblastoma Cells *Marcelo Vazquez, MD, PhD, Loma Linda University Medical Center*
3:50 pm	Impact of Planning Technique on Monte Carlo–Based Biological Dose Models in the Treatment of Pediatric CNS Malignancies with Spot-Scanning Proton Therapy *Cole Kreofsky, MD, Mayo Clinic*
4:00 pm	Radiobiological Issues and Clinical Trials *Piero Fossati, MD, CNAO*
5:00 pm	Radiobiology Panel Discussion
6:30–9:00 pm	**Memphis Blues at the Beale Street Landing (*hors d'oeuvres*)***
Monday, October 24	
7:30–8:40 am	**Sunrise Session 1: Adult**
7:30 am	Adult Gliomas *Paul Brown, MD, MD Anderson Cancer Center*
8:10 am	Adult Meningiomas *Vinai Gondi, MD, Northwestern Medicine Chicago Proton Center*
8:45–9:00am	**Welcome and Opening Remarks**
9:00–9:30 am	**Emerging Indications Session** *Session Chairs: Hesham Gayar, MD, Karmanos Cancer Institute, and James Metz, MD, University of Pennsylvania*
9:00 am	Three Fraction Skin-Sparing Pencil-Beam Scanning Proton Accelerated Partial Breast Irradiation *Robert W. Mutter, MD, Mayo Clinic*
9:10 am	Proton Treatment Patterns in the US, 2012–2015 *William Hartsell, MD, Northwestern Medicine Chicago Proton Center*

9:20 am	The Provision Experience Treating More Than 150 Breast Cancer Patients with Pencil Beam Scanning *Marc Blakey, MS, Provision Center for Proton Therapy*
9:30–10:10 am	**The Cutting Edge Session: Adaptive Particle Therapy** *Session Chairs: Nancy Mendenhall, MD, University of Florida, and Jeffrey Bradley, MD, Washington University/Barnes Jewish Hospital*
9:30 am	Pros and Cons of Proton Therapy for Thoracic Malignancies *Jeffrey Bradley, MD, Washington University/Barnes Jewish Hospital*
9:50 am	Use of Prompt Gamma for proton Range Verification *Alexander Lin, MD, University of Pennsylvania*
10:10–10:40 am	**Break**
10:40–11:40 pm	**Original Contributions Session I** *Session Chairs: Marcio Fagundes, MD, Miami Cancer Institute, and Andrew Lee, MD, MPH, Texas Center for Proton Therapy*
10:40 am	The Role and Challenges in Using Rectal Spacer Hydrogel in Proton Therapy for Prostate Cancer *Marcio Fagundes, MD, Miami Cancer Institute*
10:50 am	Comparison of Hydrogel Spacer and Rectal Immobilization on Intra-fraction Motion Equivalence Using Image Guidance Prostate Proton Therapy *Rachel Rendall, ASRT, Northwestern Medicine Chicago Proton Center*
11:00 am	Efficacy and Toxicity of Proton Therapy for Prostate Cancer Patients with Unilateral Hip Prosthesis *R. Charles Nichols, University of Florida*
11:10 am	Reduction in Rectal Dose in Prostate Cancer Patients Using Hydrogel Spacer During Proton Therapy *Jesse Conterato, BA, Northwestern Medicine Chicago Proton Center*
11:20 am	Effect of Interfractional Anatomical Changes on Proton Therapy *James Stuckey, Rhodes College*
11:30 am	Acute Side Effects of Proton Beam Therapy for Uveal Melanoma *Michael Rutenberg, MD, PhD, University of Florida*
11:40 am–1:00 pm	**Lunch at the Domino's Event Center***
1:00–2:00 pm	**Original Contributions Session II** *Session Chairs: Carl Rossi Jr, MD, Scripps Proton Therapy Center, and Brian Chon, MD, ProCure Proton Therapy Center, New Jersey*
1:00 pm	Proton Therapy Maintains or Improves Performance Status in Reirradiation Patients *Stacey Schmidt, CMD, Northwestern Medicine Chicago Proton Center*
1:10 pm	Race Does Not Affect Tumor Control, Toxicity, or Patient-Reported Quality of Life after Proton Therapy for Prostate Cancer *Curtis Bryant, MD, MPH, University of Florida*
1:20 pm	Dosimetric Comparison of Breast Boost Contribution to Composite Breast Dose in the Setting of Oncoplastic Reconstruction *Julie Bradley, MD, University of Florida*
1:30 pm	On-board Cone-Beam Computed Tomography with Spot-Scanning Proton Therapy System is Useful for Considering of Replanning in Head and Neck Region: Case Presentation

	Kazuhiko Tsuchiya, MD, PhD, Hokkaido University
1:40 pm	9DOF Geometric Calibration of a Couch-Mounted Imaging System Installed in Image-Guided Ion Beam Therapy Using a Novel Cylindrical Ball Bearing Phantom *Andrea Zechner, MSc, MedAustron*
1:50 pm	Dosimetric Impact of Using a Novel Robust, Continuous, Delivery-Efficient Spot-Scanning Proton Arc Therapy in Treating Stage III Non–Small-Cell Lung Cancer Patients *Xiaoqiang Li, PhD, Beaumont Health System*
2:00–3:30 pm	**Poster Session and Break** *Session Chairs: David Followill, PhD, MD Anderson, and Jonathan Ashman, MD, PhD, Mayo Clinic*
3:30–4:30 pm	**General Assembly**
6:30–9:00 pm	**Dinner at the National Civil Rights Museum***
Tuesday, October 25	
7:30–8:45 am	**Sunrise Session 2: Lung**
7:30 am	Proton Therapy for Lung Cancer: NSCLC & SCLC *Charles Simone II, MD, University of Pennsylvania*
7:55 am	Proton Therapy for Other Thoracic Malignancies: Thymoma & Lymphoma *Bradford Hoppe, MD, MPH, University of Florida*
8:20 am	Motion Management in Thoracic Malignancies *Stella Flampouri, PhD, University of Florida*
9:00–9:50 am	**Clinical Trials Update I** *Session Chairs: Nancy Mendenhall, MD, University of Florida, and Alexander Lin, MD, University of Pennsylvania*
9:00 am	Trials and Tribulations *Nancy Mendenhall, MD, University of Florida*
9:10 am	Impact of Unfavorable Factors on Outcomes among Inoperable Stage II-IV Non-Small Cell Lung Cancer Patients Treated with Proton Therapy *James Zhu, MD, PhD, University of Florida*
9:20 am	Proton Therapy Centers' Participation in NCI's NCTN Clinical Trials: The Role of IROC Houston QA Center *Paige Taylor, MS, MD Anderson Cancer Center*
9:30 am	Insurance Approval, a Major Challenge for Accruing Patients to a Randomized Controlled Trial of Proton Versus Photon Therapy in Patients with Oropharyngeal Cancer *Steven Frank, MD, MD Anderson Cancer Center*
9:40 am	Treatment Algorithm to Minimize Radiation Exposure to Organs at Risk and Optimize Target Coverage Consistently Favors Proton Therapy *Julie Bradley, MD, University of Florida*
9:50–10:30 am	**Break**
10:30–11:20 am	**Clinical Trials Update Session II** *Session Chairs: Steven Frank, MD, MD Anderson Cancer Center, and William Hartsell, MD, Northwestern Medicine Chicago Proton Center*
10:30 am	Preliminary Toxicity of a Trial of Escalated Dose Proton Radiotherapy for Patients

	with Initially Unresectable Pancreatic Adenocarcinoma *R. Charles Nichols Jr., MD, University of Florida*
10:50 am	Toxicity Outcomes in Breast Cancer Patients Receiving Reirradiation with Proton Therapy *Lisa McGee, MD, Northwestern Medicine Chicago Proton Center*
11:00 am	Pulmonary Toxicity Following Proton Therapy to the Thorax Among Lymphoma Patients *Ronica Nanda, MD, University of Florida*
11:20 am	Image-Guided Hypofractionated Proton Therapy in the Management of Centrally Located Early-Stage NSCLC *Bradford Hoppe, MD, MPH, University of Florida*
11:20 am–12:30 pm	**Lunch at the Domino's Event Center***
12:30 –1:30 pm	**Keynote: Why Do We Need Carbon Ions?** *Introduction: Eugen Hug, MD, ProCure Proton Therapy Center, and MedAustron Ion Therapy Center* *Speaker: Marco Durante, PhD, University of Trento*
1:30–2:30 pm	**Original Contributions Session III** *Session Chairs: Bradford Hoppe, MD, MPH, University of Florida, and Oren Cahlon, MD, Memorial Sloan-Kettering*
1:30 pm	Trends in Cardiac Biomarkers Following Adjuvant Proton Therapy for Breast Cancer *Babita Jyoti, MD, Ackerman Cancer Center*
1:40 pm	Commissioning of Spot Measurement Equipment in a Light Ion Beam Therapy Facility: the MedAustron Experience *Virgile Letellier, MSc, MedAustron*
1:50 pm	Proton Lung Treatments in the Seated Position: Development and Installation of a Vertically Positioned CT Scanner for Imaging Thorax Patients *Draik Hecksel, PhD, Northwestern Medicine Chicago Proton Center*
2:00 pm	Seamless Spot-Scanning Proton Beam Therapy for Unresectable, Large (> 25 cm) Soft Tissue and Bone Sarcomas: Two Case Reports *Takayuki Hashimoto, MD, Hokkaido University*
2:10 pm	Changes in Serum Testosterone 60 Months after Proton Therapy for Localized Prostate Cancer *R. Charles Nichols Jr., MD, University of Florida*
2:20 pm	Increasing Energy Layer Spacing in PBS plans to Reduce Beam Delivery Time while Maintaining Clinical Goals and Robustness *Hazel Ramirez, Northwestern Medicine Chicago Proton Center*
2:30–3:20 pm	**Poster Session and Break**
3:20–4:10 pm	**Pediatric Session I** *Session Chairs: Torrun Yock, MD, Harvard Medical School, and Daniel Indelicato, MD, University of Florida*
3:20 pm	Low Acute Symptom Burden of Proton Beam Therapy for Primary Brain Tumors *J. Ben Wilkinson, MD, Provision Center for Proton Therapy*
3:30 pm	Proton Beam therapy for Pediatric Patients with Rhabdomyosarcoma: A Japanese National Survey *Masashi Mizumoto, MD, PhD, University of Tsukuba*

3:40 pm	Incidence of Brainstem Necrosis Following Proton Therapy for Posterior Fossa Tumors in Children *Daniel Indelicato, MD, University of Florida*
3:50 pm	Long-Term Follow-Up After Proton Beam Therapy for Pediatric Tumors: A Single Institute Experience *Yoshiko Oshiro, MD, University of Tsukuba*
4:00 pm	A Dosimetric Comparison of Helical Tomotherapy and Intensity Modulated Proton Therapy for Selected Pediatric Cases *Elisa Coassin, MD, CRO Cancer Center*
4:15–5:15 pm	**Is Proton Therapy the Ideal Tool for Hypofractionation?** *Chair: Eugen Hug, MD, ProCure Proton Therapy Center, and MedAustron Ion Therapy Center* *Yoshiya (Josh) Yamada, MD, Memorial Sloan Kettering Cancer Center*
6:30–9:00 pm	**Gala at the Bass Pro Shop at the Memphis Pyramid***

Wednesday, October 26

7:30–8:45 am	**Sunrise Session 3: Pediatric***
7:30 am	Proton Therapy for Infants *Anita Mahajan, MD, MD Anderson Cancer Center*
7:55 am	Comprehensive Proton Therapy Immobilization Techniques for the Pediatric Population Requiring Anesthesia *Devon Barry, MS, RT(T), St. Jude Children's Research Hospital*
8:20 am	Initial Experience with Anesthesia for Infants and Young Children in Proton Therapy *Michael Rossi, DO, FAAP, St. Jude Children's Research Hospital*
9:00–10:00 am	**Pediatric Session II** *Session Chair: Anita Mahajan, MD, MD Anderson Cancer Center, and Andrew Chang, MD, ProCure Oklahoma City and Scripps Proton Therapy Center*
9:00 am	Proton Therapy for Craniopharyngioma: St. Jude-UFHPTI Collaboration *Thomas Merchant, DO, PhD, St. Jude Children's Research Hospital*
9:20 am	Realizing the Promise of Proton Radiotherapy in Medulloblastoma *Torrun Yock, MD, Harvard Medical School*
9:40 am	QMRI Analysis of PRT-Induced Structural Changes in Pediatric Medulloblastoma Survivors: Potential Predictor of Neurocognitive Trajectory *Andrew Zureick, University of Michigan Medical School*
9:50 am	Effects of Vertebral Body Sparing Proton Craniospinal Irradiation on the Spine of Young Pediatric Patients with Medulloblastoma *Brian Chou, Loma Linda University Medical Center*
10:00–10:30 am	**Break**
10:30–11:30 am	**Physics Session** *Session Chairs: Narayan Sahoo, PhD, MD Anderson Cancer Center, and Mark Pankuch, PhD, Northwestern Medicine Chicago Proton Center*
10:30 am	Characterization of a Multilayer Ionization Chamber Detector for Depth-Dose Curves, X and Y Profiles and Position Measurements of Proton and Carbon Ion Beams *Alfredo Mirandola, PhD, CNAO*

10:40 am	Small Field Proton Radiosurgery Using the Plateau Region of the Depth Dose Curve *Michael Lamba, PhD, University of Cincinnati*
10:50 am	A Fast Monolithic System for Proton Imaging *Fritz DeJongh, PhD, ProtonVDA, Inc.*
11:00 am	Evaluating the Dose and Image Quality of Proton Computed Tomography using a Filtered Backprojection Reconstruction from Monte-Carlo Cone-Beam Projection Simulations *Derek Moyer, MS, University of Cincinnati*
11:10 am	Analyzing the Effect of Range Shifter Thickness and Air Gap on TPS Dose Modeling Accuracy in Superficial PBS Proton Therapy *Robert Shirley, MS, Willis-Knighton Cancer Center*
11:20 am	The Reconstruction of the Four-Dimensional Dose Distribution in Spot-Scanning Proton Beam Therapy Using the Fiducial Marker Motion and Treatment Machine Log Data *Shusuke Hirayama, PhD, Hokkaido University*
11:30 am–11:45 am	**Closing Remarks**
12:00–2:00 pm	**PTCOG-NA Officer Meeting (closed)**

**non-educational social event*

Keynote Speaker

We are pleased to welcome **Professor Marco Durante, PhD**, Director, Trento Institute for Fundamental Physics and Applications, National Institute for Nuclear Physics (TIFPA-INFN), Department of Physics, University of Trento, Italy, as our Keynote Speaker.

Dr. Durante was appointed as the Director of the Trento Institute for Fundamental Physics and Applications (TIFPA), part of the Italian National Institute for Nuclear Physics (INFN), in April 2015. He previously served as Director of the Biophysics Department at GSI Helmholtz Center for Heavy Ion Research (Darmstadt, Germany) since 2007. He is also Professor of Physics at the University of Naples Federico II in Italy and an Adjunct Professor at Temple University in Philadelphia and at the Gunma College of Medicine in Japan.

He received his PhD in physics in 1992 and has dedicated his research efforts to the biophysics of high-energy charged particles, with applications in cancer therapy and space radiation protection. He is generally recognized as world leader in the field of particle radiobiology and medical physics and is co-author of over 300 papers in peer-reviewed scientific journals (*h*-index=38) and one patent on proton therapy (*EU patent* WO2013083333). He is currently chair of the ESA Life Sciences Advisory group and of the ESA Topical Team on Space Radiation, vice-chair of the Particle Therapy Co-Operative Group (PTCOG), member of the technical-scientific Committee of the Italian Hadrontherapy Center (CNAO) and of the Program Advisory Committee of the GANIL (Caen, France), KVI (Groningen, The Netherlands), and LNS (Catania, Italy) accelerators. Dr. Durante was President of the International Association for Radiation Research (IARR) from 2011 to 2015 and is Associate Editor in several International scientific journals (*Br J Radiol, Int J Particle Ther, Phys Med, Radiat Environ, Biophys J Radiat Res, Life Sci Space Res, JINST*).

Dr. Durante has been awarded several prizes for his outstanding contributions to charged particle biophysics, including:

- 60th Timofeeff-Ressovsky medal by the Russian Academy of Sciences
- 8th Warren K. Sinclair Award of the US National Academy of Sciences
- 2013 IBA-Europhysics award for Applied Nuclear Science and Nuclear Methods in Medicine (European Physics Society)
- 2013 Bacq & Alexander award of the European Radiation Research Society (ERRS)

Oral Presentation Abstracts

The dose weighted LET and Relative Biological Effectiveness (RBE) for DNA Double Strand Break (DSB) induction for IMPT with spot scanning pencil beam and for conventional technique using broad proton beams with patient specific aperture and compensator

Presented by Vadim Moskvin, PhD (St. Jude Children's Research Hospital)

Purpose: Dose-weighted linear energy transfer (dLET) is widely used as quantitative criteria for late effect analysis in proton therapy. New delivery techniques such as intensity modulated proton therapy (IMPT) with pencil proton beam without patient specific aperture and compensator (AC) will lead to studies focused on comparison of the later effect between IMPT and passive scattering method or uniform scanning with AC. This study presents the results of the testing of the dLET concept as a parameter in such comparison.

Methods: Particle- and energy-specific information from the independently tested Monte Carlo Damage Simulation (MCDS) was integrated into the FLUKA code systems to account for spatial variations in the RBE for protons and other light ions using an endpoint of DNA double strand break (DSB) induction. Intensity modulated proton therapy IMPT and broad beams (BB) with (AC) were simulated in the TOPAS and FLUKA code systems.

Results: Neutrons produced in the nozzle are two orders of magnitude higher for proton beam with AC in comparison to those produced from the phantom only by IMPT in the low energy part of the spectra. The fraction of the few ten of MeV protons from sequential (n,p) + (p,n) reactions increases with increasing depth beyond the Bragg peak. The proton spectra for IMPT beams at the depths beyond the distal edge contain a tail of high energy protons from neutrons generated in the phantom. The integral from the tail is compatible with the number of 5-8 MeV protons. The dose averaged energy (dEav) decreases to 7 MeV at the tip of (BP) and then increases to about 15 MeV beyond the distal edge. The computed dLET values beyond of the distal edge of the BP are 5 times larger for IMPT than for BB with the AC. Contrarily, negligible differences are seen in the RBE estimates for IMPT and beam with AC beyond the distal edge of the BP.

Conclusion: The difference in secondary neutrons spectra defines the difference between dLET from IMPT and a beam with AC. The analysis of late effects in IMPT with a spot scanning and double scattering or scanning techniques with AC may requires both dLET and RBE as quantitative parameters to characterize effects beyond the distal edge of the BP.

Pre-Clinical Study of the Effects of Duocarmycin SA and Proton Radiation on Glioblastoma

Presented by Marcelo Vazquez, MD, PhD (Loma Linda University)

Background: Glioblastoma multiform (GBM) is the most common primary brain tumor in humans with a poor prognosis, largely due to GBM being resistant to current radio- and chemotherapies. Improvements in treatment modalities for GBM are urgently needed. Particle beam therapy with protons is considered the most effective form of radiation therapy for GBM. Clinical studies have shown that delivery of DNA alkylating agents (temozolomide, TMZ) during radiotherapy increases survival rates of GBM patients, which suggest that this DNA alkylating agent can enhance the radiosensitivity of GBM. While clinically useful, TMZ is a fairly ineffective compound. The duocarmycin class of antitumor antibiotics, exemplified

by duocarmycin SA (DSA), is an exceptionally potent group of agents capable to induce a sequence-selective alkylation of duplex DNA.

Objectives: To compare the in vitro efficacy of DSA in combination with proton radiation against GBM cells and normal human lung epithelial cells (HLE). We hypothesize that DSA will function as a potent radiosensitizer against GBM.

Methods: GBM and HLE cells were irradiated with protons and/or incubated with DSA to explore the cytotoxic response at multiple time points after treatment. Each cell line was analyzed for cell toxicity by dye exclusion assay and apoptosis detection via flow cytometry to define a time-course and dose-response relationships.

Results: Experiments were performed to determine the combined effects of proton radiation and DSA against GBM and HLE cell viability. The resulting DSA-induced cytotoxicity data for both cell lines show a distinct dependence on concentration. At 0.1 nM, DSA reduced GBM cell survival by 24%, with a maximum response of 75% survival reduction with 0.5 nM of DSA. GBM cells exposed to single proton doses (3 Gy) induces a relative low decrease of cell survival (70%). In combination with 0.1 nM DSA, the level of cell surviving drops by half, to 31%. HLE cells exposed to protons and 0.1 nM DSA survived at 82%, and were unaffected by a 3 Gy dose of radiation alone.

Conclusions: This study shows that DSA at sub-nanomolar concentrations can effectively enhance the radiosensitivity of GBM cells. The differential response of these two cell lines to the action of DSA at low concentrations is promising from a toxicity standpoint.

Impact of Planning Technique on Monte Carlo-based Biological Dose Models in the Treatment of Pediatric CNS Malignancies with Spot-Scanning Proton Therapy

Presented by Cole Kreofsky, MD (Mayo Clinic)

Objectives: Spot-scanning proton therapy (SPT) is increasingly used to treat pediatric CNS tumors. Relative biological effectiveness (RBE) increases at the end of the Bragg-peak and the generalized RBE of 1.1 (compared to photons) may underestimate biologic dose (BD) at the end of the Bragg-peak. SPT can result in heavily weighted spots at unpredictable locations based on treatment planning algorithm. Our institution utilizes Monte Carlo (MC)-based BD algorithm for plan quality assurance to facilitate evaluation beam path effects. Here we describe dose distribution of 3 CNS cases treated with SPT prescribed to 5400-cGy(RBE1.1), using different planning techniques.

Methods: Pediatric CNS patients treated with SPT at our institution from June 2015-July 2016 were reviewed. Three unique cases were selected for comparison: A) CTV1=5400cGy in 30 fractions, B) CTV1=5100cGy with a simultaneous integrated boost (SIB) to 5400cGy (CTV2) in 30 fractions, and C) CTV1=5040cGy in 28 fractions followed by a sequential 2 fraction boost to 5400cGy (CTV2). For patients B & C, GTV5400=CTV5400 (CTV2) and CTV1=GTV+ 1-cm uniform expansion (anatomically constrained). Intensity modulated proton therapy (IMPT) plans were created for each patient using Eclipse (Varian Medical Systems) using a RBE of 1.1. BD was calculated from our MC-based model assuming a linear relationship between linear energy transfer and biological equivalent dose. BD and physical dose (PD) dose-volume histogram data was compared for target coverage and normal tissues. For volume reporting purposes on patients B & C, CTV1 = CTV 1-CTV2.

Results: For all 3 patients, volume of CTV1 receiving 5130cGy PD (i.e. V95% of 5400cGy) was 100%. The PD V100%(%), V105%(%), V110%(%), and V115%(%) CTV1 was 97%, 65%, 7%, 0; 100%, 41%, 2.9%, 0; and 100%, 99.2%, 39%, 0% for patients A, B, and C, respectively. The corresponding BD is 100%, 97%, 80% 43%; 99%, 99%, 60%, 0%; and 100%, 90%, 42%, 4% for patients A, B, and C, respectively. PD V100%(cc), V105%(cc), and V110%(cc) in brain outside CTV1 was 4.3, 0.5, 0; 49.0, 0.1, 0; and 19.3, 7.4, 0.1 for patients A, B, and C, respectively. Relative BD increase in brain outside CTV1 as defined by [V100%BD(cc)-V100%PD(cc)]Ã·V100%PD(cc) was 239.5%, 123.5%, and 113.5% for patients A, B, and C, respectively.

Conclusion: Biologic modeling suggests SIB technique may result in decreased BD to brain outside CTV1 while maintaining excellent (V95%=100%) PD coverage for CTV1 and CTV2 and has become the standard planning technique for low grade pediatric CNS malignancies receiving PBT at our institution.

Three Fraction Skin-Sparing Pencil-Beam Scanning Proton Accelerated Partial Breast Irradiation

Presented by Robert Mutter, MD (Mayo Clinic)

Objectives: Randomized controlled clinical trial data suggests that a commonly used ten fraction twice daily photon APBI regimen is associated with adverse cosmesis compared to whole breast irradiation. Compared with photon APBI, proton APBI reduces the dose to non-target breast tissue, making it an attractive alternative for investigation. The optimal dose and fractionation for APBI is not known. MC1532 is a multi-institutional phase II study investigating novel 3 fraction regimens for photon, catheter-based brachytherapy, and pencil-beam scanning proton (PBSP) APBI. Here, we report on techniques and preliminary planning results for skin-sparing PBSP APBI.

Methods: Eligible patients included women >= age 50 with lymph node negative, ER+ invasive ductal carcinoma or pure DCIS measuring <= 2.5 cm. For PBSP APBI, patients were simulated in the supine position with arms up using 1 mm slice thickness. The CTV included the tumor bed with a 1 cm margin and was prescribed 21.9 Gy(RBE) in three 7.3 Gy(RBE) daily fractions. The most common beam arrangement was three multi-field optimized beams. Setup uncertainty analyses included +/- 3 mm shifts in isocenter along each translation axis and +/- 3% beam range uncertainty. The skin was defined as the first 3 mm from the body surface and 1 cc was limited to 82% of prescription or more. All patients were treated on a Hitachi PROBEAT-V proton therapy system (Hitachi, Tokyo, Japan). Dosimetry was checked to an in-house GPU-based Monte Carlo system. Patients were aligned daily using a KV 2D/3D imaging system matched to surgical clips. Optical surface imaging with AlignRT (Vision RT, London, United Kingdom) was used to verify that surface positioning was within a 3 mm tolerance relative to simulation, and to monitor intrafraction motion.

Results: To date, 88 patients, median age 65 years, have been treated including nine patients with PBSP APBI. The mean volume of breast receiving 50% and 100% of prescription or more for all PBSP patients was 28% and 9%, respectively. The mean skin maximum dose and heart mean dose was 20.4 Gy and 0 Gy, respectively. Acute toxicities have included grade 1 dermatitis (n=1) and grade 1 hyperpigmentation (n=1).

Conclusions: Three-fraction skin-sparing PBSP APBI is feasible and associated with a favorable dosimetric profile.

Proton treatment patterns in the US 2012 - 2015

Presented by William Hartsell, MD (Northwestern Medicine Chicago Proton Center)

Objectives: To evaluate trends in proton therapy in the US

Methods and Materials: The NAPT (National Association for Proton Therapy) has conducted annuals surveys of active proton centers to evaluate number of patients treated, diagnoses, and complexity of treatment.

Results: For the years 2012-2014, all of the active proton centers completed the surveys (2012- 11 centers, 2013 - 14, 2014 - 16); for 2015, 14 centers have completed the surveys thus far. The most commonly treated diagnosis is prostate cancer; but the proportion has decreased from 43.4% in 2012 to 36.4% in 2015. The number of pediatric patients has gradually increased, comprising 12.7% in 2012 and 13.5% in 2015. The largest increases have been in head & neck cancers (2012 - 5.9%, 2015 - 11.3%), breast cancer (2012 - 1.7%, 2015 - 5.8%), and gastrointestinal cancers (2012 - 3.2%, 2015 - 5.7%). The proportion of patients treated for central nervous system tumors (10-11%), lung cancers (7-8%) and base of skull / skeletal tumors (3-4%) have been relatively stable.

Conclusions: The number of patients treated with protons is gradually but steadily increasing. The number of patients treated for "traditional" indications for protons - for example, pediatrics, brain, and base of skull tumors - is increasing slowly. However, there is a shift to "new" disease sites treated, especially with an increase in breast, head & neck, gastrointestinal tumors.

The Provision experience treating more than 150 breast patients with pencil beam scanning

Presented by Marc Blakey, MS (Provision Proton Center)

High skin dose has traditionally been a concern when treating with scattering and uniform scanning proton techniques, restricting the use of protons particularly in whole breast therapy. With pencil beam scanning (PBS), the whole breast can now be uniformly treated while maintaining skin dose to approximately 90% of the prescription dose.

The Provision Center for Proton Therapy (PCPT) in Knoxville, TN is a PBS only facility, and breast treatments are the second largest cohort of patients treated. To date, we have treated more than 150 breast patients, including post mastectomy chest wall with selected nodes (28%), accelerated partial breast (5%), whole breast with selected nodes (majority) after partial mastectomy (64%), bi-lateral intact breast (3%) and one breast patient with tissue expanders. For breast cases, we measure skin sparing as the dose to the proximal 5 mm of the breast which abuts the CTV. The ultimate goal is to keep the skin dose at no more than 90% of the prescription while covering the CTV with a minimum of 90% of the prescription dose. Per RTOG, the coverage goal is at least 95% of the target receiving 95% of the prescription dose. In our experience, we can provide whole breast treatment with proton therapy that delivers less dose than photon therapy to up to 2/3 of the skin abutting the target. An additional advantage of PBS is in cases when the lymph nodes (axillary, internal mammary, and supraclavicular nodes) are treated. In these cases, our proton treatments improve heart and lung sparing compared to other treatment modalities. Our breast treatments typically utilize one en-face beam at a ?30 degree gantry angle, with the patient immobilized in the supine position, and the patient's chest is angled 10 - 15 degrees using a breast board. A second beam is used if the nodes cannot be covered robustly with a

single beam. Our ongoing experience has shown that patients tolerate treatment well and are able to complete the treatment course without interruption and with minimal side effects, e.g. radio dermatitis.

We will report on the dose fractionation, immobilization and treatment planning techniques employed to allow us to treat this large variety of breast cases and the early clinical observations and tolerability of the treatments. Sharing our experience with treating this large number of breast patients will serve the proton community well.

Comparison of hydrogel spacer and rectal immobilization on intra-fraction motion equivalence using image guidance prostate proton therapy

Presented by Rachel Rendall, BS (Northwestern Medicine Chicago Proton Center)

Background: Proton therapy treatment plans are sensitive to internal and external motion due to the specific calculation of range to the target volume. Because of this, localization and immobilization of the prostate is important. At our center, the standard of prostate immobilization is through the use of an endorectal balloon (ERB) placed into the rectum. SpaceOAR (Augmenix) is a hydrogel made of polyethylene glycol intended to reduce the high dose to the rectum by acting as a spacer between the rectum and the prostate during prostate radiotherapy. In this study we evaluate the efficacy of hydrogel acting as a prostate stabilizer and the efficiencies of its use.

Material and Methods: Data was collected from 79 prostate cancer patients treated with proton therapy. All patients had 3 fiducial markers implanted perineally into the prostate to aid in target alignment for 2D kV portal imaging. 45 of the patients received 10cc SpaceOAR hydrogel as a rectal spacer. 34 patients were simulated and treated daily with a 90cc endorectal balloon.

Results: 2020 images gained during 1010 fractions were analyzed: 487 fractions in the hydrogel group and 523 fractions in the 90cc ERB group. The mean magnitude (in mm) for the hydrogel group was 1.28 (SD=0.95). The mean magnitude for the 90cc ERB group was 1.1 (SD=0.55). An ANOVA was performed to test the difference in the mean magnitude between the two groups, and this yielded statistically insignificant results (p= 0.344).

Conclusions: Based on our study, hydrogel can be used as a prostate stabilizer for proton therapy. Hydrogel proved to be just as effective as endorectal balloons to reduce intra-fraction motion. The additional benefit of hydrogel is that it is a onetime injection prior to treatment. This saves time for therapists by eliminating daily endorectal balloon preparation as well as the cost of having a balloon for each fraction. These efficiencies in conjunction to its actual use of reducing rectal dose show hydrogel as a good choice for prostate immobilization for proton therapy.

Efficacy and Toxicity of Proton Therapy for Prostate Cancer Patients with Unilateral Hip Prosthesis

Presented by Romaine Charles Nichols Jr, MD (University of Florida)

Purpose: Proton therapy for prostate cancer patients with a hip prosthesis requires field arrangements to avoid beams passing through the metallic device. These arrangements result in higher dose to the “normal” femur and delivery of dose through the bladder or rectum.

Materials and Methods: From 1/2007 through 5/2008, 4 patients unilateral hip prosthesis were treated. After a 3 year period to determine safety of this approach, from 3/2011 through 8/2014, 7 additional patients were treated.

Results: Median follow-up 26 months (8 to 97). Median age 72 years (52 to 76). Risk groups: high 2; intermediate 5; low 4. Median prostate dose 78 Cobalt Gray Equivalent (CGE) (range 78 to 82). Median seminal vesicle (SV) dose 46CGE (range 0 to 78). There were no grade 2 or higher gastrointestinal events and no grade 3 or higher urinary events. Four patients reported grade 1 rectal bleeding – 3 of whom were taking blood thinners (warfarin or apixaban) but no grade 2 or higher GI events. Excluding problems related to underlying obstructive uropathy treated with tamsulosin or temporary catheterization, there were 2 patients with grade 2 urinary events consisting of transient hematuria which resolved spontaneously. No patient experienced biochemical failure by the Phoenix criteria. Median maximum femur dose 46.4 CGE (range 34.9 to 65.1). Median mean femur dose 38.6CGE (range 12.4 to 50.2). One patient underwent uncomplicated hip replacement 7 years after proton therapy without other orthopedic events.

Conclusions: Patients with unilateral hip replacements can be safely and effectively treated with proton therapy without increased risk of toxicity or treatment failure.

Reduction in Rectal Dose in Prostate Cancer Patients Using Hydrogel Spacer During Proton Therapy

Presented by Jesse Conterato, BA (Northwestern Medicine Chicago Proton Center)

Objectives: Injection of hydrogel spacer (HS) can create space between the prostate and rectum and has been demonstrated to reduce rectal dose in men receiving intensity modulated radiotherapy for prostate cancer (CaP). Placement of HS should also reduce rectal dose in CaP patients treated with definitive proton beam radiotherapy (PBRT). This single institution review compares reduction of rectal dose using HS versus daily endo-rectal balloon (RB) in men receiving definitive PBRT for CaP.

Methods: From April 2015 to February 2016, 63 men with localized CaP had placement of HS and were treated with PBRT. This cohort was matched to a cohort of CaP patients treated with PBRT using RB (N=65) based on the following criteria: prostate cancer risk stratification and treatment era of January to December 2014. All patients completed PBRT, receiving 79.2 Cobalt Gray Equivalent (CGE) in 44 fractions. Records were retrospectively reviewed to obtain dosimetric variables assessing bladder, rectal and penile bulb doses. Dosimetric variables were compared using a two-tailed, independent t-test and calculated using Microsoft Excel.

Of the 63 patients receiving HS, PBRT was delivered for low risk (N=15), intermediate risk (N=33) and high risk (N=15) disease. PBRT targets were prostate (P) only (N=14), prostate and seminal vesicles (P+SV) (N=36) and P+SV with elective inclusion of pelvic lymph nodes (PLN) (N=13). In this cohort, median prostate size was 63.9cc (35.0-253.0cc). Of the 65 men receiving RB, PBRT was delivered for low risk (N=17), intermediate risk (N=33) and high risk (N=15) disease. PBRT targets were P only (N=15), P+SV (N=41) and P+SV with elective inclusion of PLN (N=9). In this cohort, median prostate size was 58.3cc (30.7-134.0cc).

Results: Median Rectum Eval V50 and V70 were reduced in men using HS compared to RB (21.2% vs. 16.8%, p=0.00003; 11.78% vs. 5.66%, p<0.00001, respectively). Median Rectum V81 was also reduced in men using HS compared to RB (0.02cc vs. 0.00cc, p=0.0004). There were no significant differences in median Bladder V81, V80, V50 and mean penile bulb dose.

Conclusion: HS during definitive PBRT for CaP resulted in lower rectal dose compared to RB. Additional follow-up is needed to assess rectal toxicity.

Effect of Interfractional Anatomical Changes on Proton Therapy

Presented by James Stuckey (Rhodes College)

Among treatments in radiation oncology, proton therapy leads the way in quality of treatment and life. However, because protons are particles, they are sensitive to bodily changes and fluctuations'"any change in density will impact the stopping point of the proton. This is especially important in pediatric patients since the side effects of radiation on growing tissue can hinder development and impact quality of life. In this research, we looked at the effect of daily changes in bowel gas location and body deformation in 10 randomly chosen pediatric patients with tumors in the pelvic area to see how much impact these changes had on the delivering of the prescribed dose. Cone Beam Computerized Tomography (CBCT) scans taken from each fraction were used to contour the location of the bowel gas and the body deformation for each day of treatment, and a higher quality Computerized Tomography (CT) was used for creating single field uniform dose (SFUD) plans. Before evaluating the dosimetric impact of these changes, radial Water Equivalent Thickness (WET) plots were generated using calibration curves and were included in the analysis. In general, for the dosimetric impact, it is evident that the effect on the quality of plan is highly dependent on the location of the tumor in the pelvis, with 2 patients having a greater than 8% increase in cold spot area in the planning target volume (PTV); whereas, the other 8 patients had a less than 2% increase in cold spot area in the PTV. Overall, it seems that tumors in the medial anterior section of the pelvis may be more susceptible to changes in plan quality than other tumors. However, for the majority of tumors, it seems that the use of multiple beams (especially posterior beams) for SFUD plans may help to mitigate the effect of any daily changes.

Acute Side Effects of Proton Beam Therapy for Uveal Melanoma

Presented by Michael Rutenberg, MD, PhD (University of Florida)

Purpose/Objectives: There are limited data available describing the acute side effects associated with proton beam therapy (PBT) for the definitive management of patients with uveal melanoma. We report our initial experience with acute toxicities related to PBT for uveal melanoma.

Materials/*Methods*: From 2012 to 2016, 55 patients were treated definitively for uveal melanoma with hypofractionated PBT. Tantalum fiducials were sutured onto the sclera prior to treatment planning for daily alignment. Treatment consisted of 60 CGE delivered in 15 CGE/fx on consecutive days using passive scattering PBT on a fixed beam eyeline. Prospectively recorded acute treatment related side effects within 180 days of treatment were analyzed.

Results: Median follow-up was 1.1 years (range: 0.1- 3.0 years). The median age at treatment was 60 years old (range: 26 - 94). Twenty-nine right eyes and 26 left eyes were treated; T1 = 9, T2 = 17, T3 = 17, and T4 = 12. All patients but one (iris melanoma) had disease involving the posterior uveal

structures. The median tumor size was 14.5 mm (range: 5.2 - 21.0) in maximum diameter and 6.0 mm (range: 1.2 - 13.0) in thickness. The median interval between tantalum clip placement and PBT was 13 days (range: 4 - 28). 82% had conjunctivitis and 9% had eyelid dysfunction following tantalum clip placement prior to PBT. At 6 weeks post-PBT conjunctivitis and radiation dermatitis were the most common toxicities, occurring in 49%, and 42% of patients, respectively. At 3 months, conjunctivitis, dermatitis, and epiphora occurred in 38%, 25% and 36% of patients, respectively. At 6 months, these side effects decreased in frequency (20%, 18% and 29%, respectively). There were 6 events of grade 3 toxicity consisting of eye pain (1), cataract (1), complete retinal detachment requiring surgery (1), and epiphora (3). There was one grade 4 toxicity (retinopathy) that occurred at 6 months post-PBT. One patient was enucleated 3 months post-PBT due to tumor progression, but without treatment related toxicity. There were no grade 5 toxicities. Median visual acuity for early stage tumors (T1/T2) remained stable from pre-treatment baseline to 6 months post-PBT. Median visual acuity in locally advanced tumors (T3/4) remained stable from baseline to 3 months post-treatment, however, declined at 6 months post-PBT ($p = 0.035$).

Conclusion: Hypofractionated proton beam therapy is generally well tolerated, though, 13% of patients experienced >= grade 3 acute side effects.

Proton Therapy Maintains or Improves the Performance Status in Reirradiation Patients

Presented by Stacey Schmidt, CMD (Northwestern Medicine Chicago Proton Center)

Background: Proton therapy is frequently used in patients undergoing radiation to a previously irradiated treatment site, because of the ability to spare surrounding critical tissue structures. The purpose of this study is to determine whether proton therapy to spare surrounding normal tissues can help either maintain or potentially improve the performance status of these patients.

Methods: We evaluated 105 patients who underwent reirradiation at the Northwestern Medicine Chicago Proton Center in 2015 and who were enrolled in the PCG-001-09 Registry Trial or ATOM trial. Performance statuses (PS) at the initiation of treatment and at the first follow-up appointment were recorded using the ECOG and Lansky scales.

Results: The specific treatment sites for these 105 patients included cancers of the brain, head & neck, lung, breast, metastatic tumors, and miscellaneous 'other'. Only 56 patients had both a performance status score taken at the initiation of treatment and the first follow-up visit. The other 49 included 40 patients who never returned to our center for follow-up and 9 who died prior to their first follow-up appointment. The breakdown of patients per treatment site included 8 adult CNS patients, 8 head & neck, 13 lung, 7 breast, 5 metastatic disease, and 15 were miscellaneous 'other'. Of the 8 adult CNS patients, 5 statuses remained the same, 1 improved, and 2 were worse. 6 of the 8 head/neck patients' scores remained stable and 2 improved. 11/13 lung cancer patients' scores remained stable, and 2 improved. Of the 7 breast patients, 5 patients' scores remained stable, 1 improved, and 1 was worse. Of the 5 metastatic patients, 2 patients' scores remained stable, 2 improved, and 1 was worse. Of the patients in the 'other' category, 7 patients' scores remained stable and none of these patients' scores improved. Overall, 64% of the patients had stable PS, 14% had improved PS, and only 21% worsened.

Conclusions: Overall, the majority of the evaluable patients who underwent proton therapy to a previously irradiated treatment site did demonstrate maintained or improved performance status from the initiation of treatment to their first follow-up appointment.

Race Does Not Affect Tumor Control, Toxicity, or Patient-Reported Quality of Life after Proton Therapy for Prostate Cancer

Presented by Curtis Bryant, MD, MPH (University of Florida)

Objectives: To compare 5-year biochemical control, toxicity, and patient-reported quality of life (QOL) outcomes for African American and white patients treated with proton therapy for prostate cancer.

Methods: We retrospectively reviewed the medical records of 1,066 men with clinically localized prostate cancer. Each patient was treated with definitive proton therapy between 2006 and 2010. A median radiation dose of 78 Gy(RBE) was delivered using conventional fractionation (1.8-2 Gy[RBE] per fraction). Sixty-eight men (6.4%) self-identified as African American and 998 (93.6%) men identified as white. Baseline patient and treatment characteristics were similar between the two groups with the exception of pretreatment IPSS scores and pretreatment PSA values. IPSS scores exceeded 15 in a smaller percentage of African Americans than white patients (9.6% vs. 17.1%; p=0.04). Also, pretreatment PSA values exceeded 20 ng/ml more often among African Americans than white patients (10% vs. 3.4%; p=0.006). Five-year rates of biochemical control, grade 3 genitourinary (GU) and gastrointestinal (GI) toxicity, and patient-reported QOL graded according to the EPIC scale are reported and compared between African American and white patients.

Results: Median follow-up was 5.0 years for both African American and white patients. On multivariate analysis (MVA), race was not a significant predictor for 5-year freedom from biochemical failure (HR 0.8; p=0.55). No association was found between race and grade 3 GU toxicity on MVA at 5 years (HR 2.5, p=0.10). No difference was seen in grade 3 GI toxicity between African American and white patients (0% vs. 0.6%, p=0.5). Patient-reported QOL characterized using median EPIC bowel, urinary incontinence, and irritative summary scores were not significantly different between the two groups during 5 years of follow up. African Americans had higher median sexual summary scores at two years than white patients (75 vs. 54; p=0.01), but after 5 years of follow up, the EPIC sexual summary scores were no longer significantly different (63 vs. 53; p=0.35).

Conclusions: With a median follow-up of 5 years, there were no racial disparities in biochemical control, grade 3 toxicity, or patient-reported QOL after proton therapy for prostate cancer.

Dosimetric Comparison of Breast Boost Contribution to Composite Breast Dose in the Setting of Oncoplastic Reconstruction

Presented by Julie Bradley, MD (University of Florida)

Purpose/Objectives: Tumor bed boost decreases the risk of local recurrence, but is associated with an increased rate of severe breast fibrosis. The NSABP B51/RTOG 1304 protocol recommends <= 50% of the volume of Breast PTV_Eval should receive >= 54 Gy (108% of 50Gy prescription dose). In the setting of oncoplastic reconstruction, delivery of a tumor bed boost may be challenging if the surgical closure results in displacement of the tissue that forms the lumpectomy bed. This dosimetric study

compares two boost modalities, 3D-conformal photon therapy and intensity modulated proton therapy (IMPT), in the setting of lumpectomy with oncoplastic reconstruction.

Methods: A retrospective review of 32 consecutive breast cancer patients treated with lumpectomy and oncoplastic reconstruction followed by photon whole breast radiotherapy with a photon boost was performed. Twenty-one patients received standard fractionation (50 or 50.4 Gy at 1.8-2 Gy per fraction with a 10 Gy in 5 fraction boost). Eleven patients received hypofractionation (42.4 Gy at 2.65 Gy per fraction with a 7.95 Gy in 3 fraction boost). Sixteen patients had right-sided and sixteen had left-sided breast cancer. IMPT plans were generated for the boost and summed with the photon whole breast plan (photon-proton) to allow for comparison to the photon only plan (photon-photon).

Results: The median pathologic size of the primary tumor was 1.5cm (range, 0.4-4.5cm). The median volume of the tumor bed was 230.4cc (range, 65.2-557.6cc). Target coverage was adequate in both the proton and photon boost plans (median D95=99% for both). The Breast_PTV receiving 108% of the initial dose on the composite plan (54 Gy standard fractionation, 45.8 Gy hypofractionation) was significantly reduced with the proton boost, from 72.7% with photon boost to 43.4% ($p<0.001$). Median V100% (of the total prescription dose) for Breast_PTV decreased from 31% with the photon-photon plan compared to 20.3% with the photon-proton plan ($p<0.001$). On the composite plans, the median Breast_PTV V107 was 19.5cc with a photon boost compared to 10 cc with a proton boost ($p=0.0002$). No clinically meaningful differences in heart or lung dose were identified in this cohort (median mean heart dose 1.4Gy photon-photon vs. 1.2Gy photon-proton; median lung V5 37.6% photon-photon vs. 33.9% photon-proton).

Conclusions: A proton boost plan can be considered in the setting of oncoplastic reconstruction after lumpectomy to minimize additional dose to the non-boost breast tissue. This reduction in excess breast dose may assist in diminishing the rates of breast fibrosis.

On-board cone-beam computed tomography with spot-scanning proton therapy system is useful for considering of replanning in head and neck region: case presentation

Presented by Kazuhiko Tsuchiya, MD, PhD (Hokkaido University)

The dose distribution of proton beam is more sensitive to changes in tumor size, surrounding density change such as air or water in the head and neck region compared to photon therapy. And such changes could cause the underdosage to the tumor and unexpected high dose to the organ at risks. CT scans are used for evaluating these changes in many institutions and when significant dosimetric changes are observed, replanning is considered. But the timing of these CT scans are unsettled. In our institution, the cone-beam computed tomography (CBCT) are mounted on the spot-scanning dedicated proton beam gantry. By using this system, we acquire on-board CBCT images after patients' set-up at least once a week in head and neck region and if noticeable changes are observed, we obtain CT images and superimpose the original treatment plan on it and re-calculate and evaluate the dose distribution whether replanning is required. We present two impressive cases which this process was useful. Case 1: 54 years old woman with recurrent adenoid cystic carcinoma of hard palate (rT4b). Prescribed dose was 56GyE/28fr. At 40GyE/20fr, tumor shrinkage was observed on CBCT scan image and the maximum dose to the brain stem was thought to be high if treated with original treatment plan and replanning was made. Case 2: 37 years old man with adenoid cystic carcinoma of nasal cavity

(cT4N0M0). Prescribe does was 65GyE/26fr. Replannings were needed due to the tumor growth and shrinkage during treatment in this patient.

9DOF geometric calibration of a couch-mounted imaging system installed in image-guided ion beam therapy using a novel cylindrical ball bearing phantom

Presented by Andrea Zechner, MS (MedAustron)

Image guidance during highly conformal radiotherapy requires accurate geometric calibration of the moving components of the imager. Due to limited manufacturing accuracy and gravity-induced flex, an X-ray imager's deviation from the nominal geometrical definition has to be corrected for. For this purpose a ball bearing phantom applicable for nine degrees of freedom (9-DOF) calibration of a novel couch-mounted Cone-Beam Computed Tomography (CBCT) scanner was designed and validated. The flat panel imaging system was calibrated for 9DOF via ground-truth fiducials embedded in the treatment couch.

For the phantom design three different methods to distribute markers on the phantom cylinder surface were investigated. Projection images of the phantom incorporating the CBCT scanner's geometry were simulated and analysed with respect to uniform marker distribution and intra-marker distance. A phantom prototype with a marker distribution based on the Golden section was manufactured and validated by a series of flexmap calibration measurements and analyses of the couch-mounted CBCT scanner with independently moveable source and detector arms. Fiducials that are implanted in the treatment couch serve as the ground truth coordinates. Their manufacturing tolerances are in the submillimetre range. Hence, the geometric calibration of the imaging system is done via the couch fiducial structure set by transforming it in the CBCT scanner's coordinate system. The transformation parameters are applied to the phantom structure set. After the calibration of the imaging system the fin al positioning accuracy relative to the couch table top is better than 1mm (3D vector) and 0.2 °.

A novel flexmap calibration phantom intended for 9DOF was developed. The ball bearing distribution based on the Golden Section was found highly advantageous. A method to determine the correct transformation for the flexmap phantom structure set was derived in order to obtain a 9DOF geometric calibration of the imaging system and the table top coordinate system. The calibration results for the CBCT scanner are satisfying and provide the basis for further 3D reconstruction developments and accurate patient positioning.

Dosimetric impact of using a novel robust, continuous, delivery-efficient Spot-Scanning Proton Arc Therapy in treating stage III non-small-cell lung cancer patients

Presented by Xiaoqiang Li, PhD (Beaumont Health System)

Purpose: Spot-Scanning Proton Arc therapy (SPArc) is a novel form of intensity modulated proton therapy (IMPT) optimization that generates robust, continuous, delivery-efficient spot scanning proton arc therapy plans. The goal of this study is to dosimetrically evaluate SPArc plans with multi-field robust optimized IMPT (RO-IMPT) plans for stage III non-small-cell lung cancer (NSCLC) patients.

Methods and Materials: The SPArc optimization algorithm was implemented into worst-case scenario robust optimization via integrating control point re-sampling; energy layer re-distribution, filtration, and re-sampling. The feasibility of such technique was evaluated using three patients with stage IIIA or IIIB

NSCLC. Both SPArc and RO-IMPT plans were generated using the robust optimization with ?3.5% range and 5mm setup uncertainties in RayStation, to achieve an optimal coverage with 99% of internal target volume (ITV) receiving 70 Gy (RBE) in 35 fractions. Dose-Volume-Histograms (DVHs) of target volume and Organs-at-Risk (OARs) were analyzed. Statistical analysis was evaluated with 2-sided paried t test. Total delivery time was compared based on 1 RPM for a full gantry rotation, 2ms spot switching time, 1nA beam current, 0.01 minimum spot monitor unit, and energy-layer-switching-time (ELST) from 0.2 to 4 seconds.

Results: Both SPArc and RO-IMPT plans achieved similar target volume coverage and plan robustness for all patients, while SPArc plans could significantly reduce integral dose and dose to normal lung. Specifically, SPArc plans reduced the averaged integral dose by 10.3% ($p = 0.03$) compared with RO-IMPT plans. The average V5, V10, V20, and mean lung dose for SPArc plans were 23.5%, 18.3%, 14.2%, and 9.2 Gy(RBE). While comparing to RO-IMPT plans, SPArc reduced the average V5, V10, V20, and mean lung dose by 4.8% ($p < 0.01$), 5.1% ($p = 0.03$), 3.6% ($p < 0.01$), and 1.7 Gy(RBE) ($p < 0.01$) respectively. In other OARs, such as spinal cord, heart, esophagus, SPArc plans achieved either superior or equal dosimetric parameters compared with RO-IMPT plans. The average total estimated delivery time was 151.9s, 289.1s, 800.1s based on ELST of 0.2s, 1s, and 4s for SPArc plans, compared with the respective values of 181.1s, 251.5s, 515.5s for RO-IMPT plans. Hence, SPArc plans could potentially achieve similar or faster delivery time when using a shorter ELST in the modern proton machine.

Conclusion: SPArc is the first robust and delivery-efficient proton spot-scanning arc therapy technique which could potentially be implemented into routine clinical practice to ultimately improve the treatment outcome in patients with locally advanced stage NSCLC.

Impact of Unfavorable Factors on Outcomes among Inoperable Stage II-IV Non-Small Cell Lung Cancer Patients Treated with Proton Therapy

Presented by James Zhu, MD, PhD (University of Florida)

Purpose/Objective: Clinical trials evaluating proton therapy (PT) for locally-advanced non-small cell lung cancer (LA-NSCLC) have been slow to accrue. We investigated outcomes in patients with LA-NSCLC treated with PT.

Methods: From May 2008 through July 2015, 102 patients with unresectable stage II-IV NSCLC received PT. Unfavorable factors included age >80 years, stage IV, weight loss >5% in 1 month, performance status (PS) >=2, FEV1 <1.0 or oxygen dependency, prior lung cancer or lung surgery, prior second cancer within 3 years, prior chest radiotherapy, and other severe comorbidities listed as clinical trial ineligibility criteria. 92 patients received 1.8-2Gy(RBE)/fraction to a median dose of 70Gy(RBE). 10 others received hypofractionation (>= 2.5Gy[RBE]/fraction). Overall survival (OS) and progression-free survival (PFS) were calculated with the Kaplan-Meier method. The impact of unfavorable factors was analyzed in univariate and multivariate Cox regression models. Median follow-up for living patients was 25.2 months.

Results: Of 102 patients, 28% were favorable-risk (0 factors), 40% had 1 unfavorable factor, 23% had 2 factors, and 9% had >=3 factors. 69% of patients were age >=65. More patients were favorable-risk

among those <65 than >=65 years (47% vs 20%; p=0.0087). More favorable-risk patients received concurrent chemoradiation than unfavorable-risk patients (100% vs 75.7%; p=0.01).

Among 92 patients treated with standard fractionation, the 2- and 3-year OS were 52% and 33% for favorable-risk and 40% and 31% for unfavorable-risk patients. The 2-year PFS rate was 24% for favorable-risk and 37% for unfavorable-risk patients. There were no significant differences in OS or PFS among patients with and without unfavorable factors. No unfavorable factor had a significant impact on OS, except prior cancer diagnosis (p=0.036). In a subset analysis of stage III-IV patients, PS>=2 adversely impacted OS (p=0.011).

Three grade 3 toxicities were found in favorable-risk patients (1 esophagitis, 1 pneumonitis, 1 late pulmonary fibrosis). Seven grade 3 toxicities were found in unfavorable-risk patients (1 esophagitis, 1 pneumonitis, and 5 pleural effusion). 1 unfavorable-risk patient developed grade 4 pulmonary stricture.

Conclusions: Most patients treated with PT for LA-NSCLC have unfavorable risk factors. These patients had similar outcomes to favorable-risk patients. Enrollment in future trials may improve if eligibility is less restrictive.

Proton Therapy Centers' Participation in NCI's NCTN Clinical Trials: The Role of IROC Houston QA Center

Presented by Paige Taylor, MS (IROC Houston, UT MD Anderson Cancer Center)

Purpose: To give an overview of the clinical trial participation of proton therapy centers in cooperative group clinical trials.

IROC Houston, in conjunction with the other IROC offices, coordinates the approval and credentialing of proton therapy centers for participation in NCI-funded clinical trials. The approval process requires each institution to complete an annual output check, a facility questionnaire, baseline phantom irradiations, electronic data transfer, and an on-site audit. Cooperative group protocols may require additional credentialing steps, such as IGRT credentialing, additional phantom irradiations, or knowledge assessments.

To date, IROC Houston has analyzed over 110 phantoms for approval and credentialing, performed 420 remote output checks, and conducted 27 on-site audits (each delivery modality requires separate approval, so several institutions have been audited twice as they implement new technology). IROC Houston has approved 18 proton therapy facilities to participate in NCI protocols, with several more proton centers currently working to complete the approval steps. Currently 12 of the 18 approved proton facilities have pencil beam scanning, indicating a shift away from passive scatter beams.

While 18 proton therapy centers have been approved for clinical trial participation, only 11 of these facilities have actually completed the required credentialing to enroll patients on NCI-funded protocols. IROC has credentialed proton therapy centers to participate in five NRG Oncology protocols and five COG protocols. Two cooperative group trials involve randomization between a photon arm and a proton arm: RTOG 1308, a lung protocol, and NRG BN001, a brain protocol. These two protocols have the largest number of proton centers credentialed to participate. IROC has credentialed 9 proton centers for

RTOG 1308, and of those, 7 centers have enrolled patients. 10 proton centers have been credentialed for NRG BN001, and of those, 7 centers have enrolled patients.

Proton therapy centers are showing interest in clinical trials when they first treat patients, but over a third have not pursued participation in protocols. It is imperative that the clinical trial PIs work in conjunction with the IROC offices to encourage proton facility participation in the NCI-funded protocols for the success of each trial. .

Insurance approval, a major challenge for accruing patients to a randomized controlled trial of proton versus photon therapy in patients with oropharyngeal cancer

Presented by Steven Frank, MD (MD Anderson)

Background: Intensity modulated proton therapy (IMPT) has shown promising outcomes in retrospective studies for the treatment of oropharyngeal cancer (OPC) patients, with similar tumor control rates and survival but lower toxicity compared to intensity modulated photon therapy (IMRT). However prospective confirmation is needed and a randomized phase II-III controlled trial is currently ongoing. The aim of this report is to describe the current accrual of the trial, and discuss the challenges faced in the accrual of patients.

Methods: Adult patients with biopsy proven stage III-IV OPC treated with definitive chemoradiation are randomized (1:1) to IMPT or IMRT. A total dose of 70 Gy is delivered in 33 fractions to the gross tumor, using a relative biologic effectiveness of 1.1 for the IMPT arm, and subclinical disease is treated to 56-63 Gy. A total of 160 patients (80 in arm) is required for the Phase II part. This trial was initiated at MD Anderson Cancer Center and is now opening in multiple proton therapy facilities.

Results: Between September 2013 and August 2016, a total of 593 non-metastatic OPC patients have been seen at MD Anderson Cancer Center. One hundred and twenty two patients were included in the trial and randomized (20.6%); 62 were allocated to IMPT and 60 to IMRT. Of the 62 patients randomized to IMPT, only 24 (39%) had immediate insurance approval, while 38 (61%) were initially denied. Of the patients initially denied insurance, 13 were approved after the appeals process, while the remaining 25 patients (40% of the randomized patients) were eventually denied insurance coverage for IMPT. Of those 25, 15 (24% of the randomized patients) could not be treated according to their randomization arm, thus dropping out of the trial while 10 eventually decided to pay for IMPT out of pocket. Five of the IMRT patients withdrew consent and were treated with IMRT closer to their home or with IMPT outside of the trial.

Conclusions: Although challenging, this early report shows that conducting a proton versus photon randomized trial is feasible. Insurance denial is the most prevalent reason for not being treated according to randomization arm. These patient dropouts will necessitate an increase in the phase III sample size in order to maintain the statistical power. Obtaining insurance approval for patients included in clinical trials investigating the difference between approved treatment technologies would greatly improve the ability to include patients and allow large trials to be conducted.

Treatment algorithm to minimize radiation exposure to organs at risk and optimize target coverage consistently favors proton therapy

Presented by Julie Bradley, MD (University of Florida)

Purpose: To assess the role of routine comparative dosimetry for proton therapy (PT) and conventional radiotherapy (CRT) for women with breast cancer and report acute toxicity with PT.

Methods: Between 2012 and 2015, 39 women (stage IA-IIIC) enrolled on a prospective registry with plans for both PT and CRT designed. Median age was 60 years (range, 37-86). Twenty women underwent lumpectomy and 19 mastectomy. Nine women had right-sided and 30 had left-sided cancer. Treatment targets (clinical target volumes for breast/chest wall, supraclavicular, axillary, internal mammary node [IMNs]), and organs at risk were delineated on CT, and PT and CRT plans were developed. In total, 90% of women received comprehensive regional nodal treatment. Acute toxicity was prospectively recorded using CTCAE v4.0. Wilcoxon signed-rank sum test compared the dose-volume parameters.

Results: Median follow-up was 2.1 years (range, 0.2-3.6). For all patients, the PT plan better met the dosimetric goals and was used for treatment. PT alone was used for 29 patients (17 post-mastectomy, 12 post-lumpectomy) and combined proton-photon treatment was used in 10 (2 post-mastectomy, 8 post-lumpectomy). Breast/chest wall coverage was adequate with both modalities (V47.5=95.5% for PT vs 91.5% for CRT; p=0.33). PT improved coverage of the level II axilla (median D95, 48.8 Gy [minimum, 44.7 Gy] with PT vs. 46.5 Gy [minimum, 39.2 Gy] with CRT; p=0.006). IMN coverage was also improved with PT (median D95, 49.3 Gy) compared to CRT (median D95, 45.9 Gy; p=0.0002). PT reduced heart and lung dose in all patients. Median mean heart dose decreased from 3.8 Gy with CRT to 0.5 Gy with PT (p<0.0001) and median maximum dose to the left anterior descending artery (LAD) decreased from 43.9 Gy to 16 Gy (p=0.0003). Median ipsilateral lung V20 and V5 measured 13.2% and 21.5% for PT compared to 32.4% and 56% for CRT, respectively (p<0.0001).

Grade 3 acute toxicity included dermatitis in 6 patients (15%) and grade 3 breast cellulitis during week 4 of PT in 1 patient. No grade 4+ toxicities developed. Dermatitis resolved by 1 month after PT for all but 1 patient who developed cellulitis after PT (grade 2).

Conclusions: Comparison of PT and CRT plans consistently results in improved dosimetric parameters with PT, including decreased dose to the whole heart, LAD, and ipsilateral lung, while simultaneously maintaining or improving target coverage. Comparison PT plans during the planning process may help determine which patients would derive significant benefit from this modality.

Preliminary Toxicity of a Trial of EscalatedDose Proton Radiotherapy for Patients with Initially Unresectable Pancreatic Adenocarcinoma

Presented by Romaine Charles Nichols Jr, MD (University of Florida)

Objective: Review preliminary toxicities for the first patients treated on a trial of dose escalated proton radiotherapy with elective nodal irradiation for patients with unresectable, borderline resectable, or medically inoperable pancreatic adenocarcinoma (UFHPTI PC04 Trial).

Methods: The UFHPTI PC04 trial was activated on 3/31/2016. By 8/12/2016, five patients had completed radiotherapy. Protocol therapy delivers a dose of 40.50Gy(RBE) in 18 fractions to an initial PTV volume (PTV1) including: an internal gross tumor volume (iGTV); and an elective nodal volume consisting of a 2cm expansion around the most proximal 1cm of the celiac artery and the most proximal 2.5cm of the superior mesenteric artery. A second volume (PTV2) including the iGTV receives an additional

22.50Gy(RBE) in 10 fractions subject to normal tissue constraints. Normal tissue constraints for the duodenum, stomach, and bowel space match the constraints of the NRG 1201 protocol. Patients receive capecitabine chemotherapy 1000mgPO BID on radiotherapy treatment days. Patients may receive chemotherapy or other systemic therapy prior to protocol therapy.

Results: Median age of treated patients is 79 years (range 71 to 88); 3 males, 2 females; T4 - 2 , T3 - 3; There were no grade 3 toxicities reported. Grade 2 toxicities were experienced by two patients. One patient experienced abdominal discomfort and weakness related to ascites which developed during the third week of treatment. One patient noted grade 2 dermatitis without moist desquamation in the final week of radiotherapy. Two patients experienced interruptions in treatment. One patient with ascites required a 10 day break for paracentesis and radiotherapy replanning. One patient was hospitalized with urosepsis unrelated to protocol therapy but was able to complete radiotherapy after a 27 day break. Median weight change from the first to sixth week of treatment was -3.6lbs (range +12.3 to -14.2).

Conclusions: Although longer term follow up is required, the lack of acute treatment related toxicity for patients treated on this protocol is encouraging. We continue to enroll patients on this trial. An update will be available at PTCOG-NA in October, 2016.

Toxicity Outcomes in Breast Cancer Patients Receiving Reirradiation with Proton Therapy

Presented by Lisa McGee, MD (Northwestern Medicine Chicago Proton Center)

Purpose: To assess toxicity of reirradiation with proton therapy (PT) in breast cancer patients.

Methods and Materials: From 2012-2015, 17 breast cancer patients received reirradiation with PT at a single institution. Patients were included if they had a history of prior thoracic radiotherapy (RT) and had indications for reirradiation to the postmastectomy chest wall and regional lymph nodes (LN) for a primary (N=1) or recurrent (N=16) breast cancer diagnosis. Indications for inclusion of LN included lymph node positive disease (N=9) or inability to surgically assess the axilla (N=8). 7 patients had immediate reconstruction prior to initiation of PT.

Prior RT characteristics include the following: 40 Gy to a mantle field for Hodgkin Lymphoma (N=1), RT to the intact breast for initial breast cancer diagnosis (N=15), and partial breast RT (N=1). Median initial RT dose was 60 Gy (34-70 Gy). Median time interval between courses of RT was 12.1 years (3-28.4 years).

Reirradiation was performed with uniform scanning PT. Median PT dose was 50.11 (45.1-76.31) cobalt gray equivalent (CGE). 3 patients had gross disease at PT initiation. Toxicity was assessed prospectively per CTCAE v. 4.0 at baseline, weekly during PT, 2 weeks and 4 weeks following PT and then every 6 months.

Results: Median follow-up was 8 months (2-39 months). At the time of last follow-up all patients had locoregional control. One patient developed distant metastases 17 months following PT.

Acute skin toxicity occurred in all patients; grade 1 (N=4), grade 2 (N=12) and grade 3 (N=1). Grade 1 esophagitis occurred in 11 patients; grade 2 (N=4). Grade 2 chest wall pain occurred in 6 patients; grade 3 (N=1). The patient with grade 3 skin toxicity and chest wall pain had diffuse moist

desquamation which peaked 2 weeks post-PT. She had a long standing history of allergies to multiple skin creams; skin desquamation and pain resolved when she stopped using her skin care regimen.

One woman experienced rib fracture 18 months post-PT, receiving a cumulative dose of 111 CGE. Pneumonitis requiring steroid treatment occurred in 1 woman 7 months post-PT. 2 women reported clinical lymphedema at last follow-up. 1 woman reported a non-healing wound at last follow-up; this patient started PT prior to complete wound healing after surgery due to the development of dermal lymphatic gross recurrence.

Conclusions: Reirradiation with PT in breast cancer patients appears to have acceptable toxicity. Longer follow-up is needed.

Pulmonary toxicity following proton therapy to the thorax among lymphoma patients

Presented by Ronica Nanda, MD (University of Florida)

Background/Purpose: Advanced radiation technologies, such as IMRT and proton therapy, have been introduced into the management of lymphoma over the last decade in an effort to reduce risk of late toxicities, specifically cardiac and secondary cancers. However, clinical outcomes and toxicities from these treatments aren't well understood and recent reports have demonstrated relatively high rates of grade 3 pneumonitis with IMRT of 7%. We therefore examine the rates of radiation-related pulmonary and other toxicities for patients treated with PT for lymphomas of the mediastinum and/or axilla.

Methods: Between September 2009 and April 2016, 59 patients with lymphoma involving the thorax received proton therapy and enrolled on an IRB approved outcomes tracking protocol at University of Florida. Patients were prospectively evaluated using a computerized toxicity assessment form that incorporated CTCAE version 4.0 toxicities for cough, dyspnea, hypoxia, pneumonitis, pulmonary fibrosis, and effusion weekly during treatment and at follow up. Additionally, patient medical record data between visits was evaluated retrospectively for additional toxicities. For the purposes of this study, acute effects were those occurring within 6 months of completing radiation therapy, while late effects were those occurring more than 6 months after radiation therapy.

Results: There were 31 pediatric and 28 adult patients (median age: 21 years); median follow up was 24.1 months (range 1-82 months). The median number of CTCAE vs4 toxicity assessments was 7 (range 4-28). The mean dose delivered was 30.6 CGE (range 15- 45 CGE). Fifty patients had Hodgkin lymphoma and 9 patients had NHL with 55 patients with mediastinal involvement. 11 patients were treated for relapsed or refractory disease and 7 patients underwent ASCT.

Twenty-one patients developed acute grade 1 and two patients (3.3%) developed acute grade 2 pulmonary toxicity. The grade 2 toxicities were cough in one patient who was treated to 45 CGE for refractory disease after chemotherapy and dyspnea in another patient with concomitant atrial myxoma who underwent resection prior to chemotherapy. Late grade 1 pulmonary toxicities were seen in 27 patients and late grade 2 toxicity was seen in 1 patient (pneumonitis with symptomatic cough treated to 39.6 CGE due to partial response after chemotherapy). Eight patients developed acute grade 2 esophagitis. There was no grade 3 or higher acute or late toxicities.

Conclusions: No significant pulmonary toxicity from proton therapy was seen among lymphoma patients treated to the thorax. Longer follow up and larger patient cohort is needed to confirm these results.

Image-Guided Hypofractionated Proton Therapy in the Management of Centrally Located Early-Stage NSCLC

Presented by Bradford Hoppe, MD (University of Florida)

Background: We investigated outcomes from delivering hypofractionated proton therapy (PT) among patients with centrally located stage I NSCLC.

Methods: From 2009 through 2015, 16 patients were treated for medically inoperable centrally located de novo (n=12) or relapsed (n=4) stage I NSCLC (IA, n=5; IB, n=11) with image-guided hypofractionated PT on an IRB-approved outcomes tracking protocol (median age, 69 years). Centrally located tumors were those within 2 cm of the proximal bronchial tree or heart. Patients underwent 4D CT simulation following fiducial marker placement and an iGTV was contoured per the 10 phases of the scan (median, 15.5 cc; range 6-56 cc). Initially, a 5-mm margin was added to make an ITV but was eliminated in 2014, followed by a 5-mm margin for the PTV (median, 78.5cc; range 32-211cc). Daily image-guidance was done using fiducial markers and double exposure of orthogonal kv imaging at the peaks of inspiration and expiration. Patients were all treated with 60 Gy(RBE) (6 Gy[RBE]/fraction x 10 fractions) utilizing pre-defined dose constraints. Patients were evaluated by a physician and assessed for CTCAEv4 toxicities weekly during treatment, at 1 month after treatment, then every 3 months for 2 years, and then every 6 months until 5 years with a CT or PET/CT. Overall survival, progression-free survival, local control, regional control, and control of distant metastases were evaluated using the Kaplan-Meier method.

Results: Median follow-up for the cohort was 44 months (range, 4-67). The 3-year progression-free survival and overall survival rates were 41% and 84%. The median progression-free and overall survival were 28 and 60 months. The 3-year local (ipsilateral lobe), regional, and distant control rates were 89%, 77%, and 74%. Four patients died with disease and 1 from complications of pneumonia 52 months after treatment. Seven patients developed a recurrence, including 5 distant, 3 regional, and 1 in the ipsilateral lobe at the edge of the treatment field. Five received salvage radiation for the recurrences using either SBRT (n=2) or standard fractionated proton therapy +/- chemo (n=3). Three have had no evidence of disease for >1.5 years.

One grade 3 toxicity occurred in a patient who developed a grade 3 bronchial stricture (PTV, 211cc) requiring hospitalization and stent. .

Conclusion: Image-guided hypofractionated PT for centrally located stage I NSCLC provides promising local control and long-term survival with acceptable toxicity.

Trends in cardiac biomarkers following adjuvant proton therapy for breast cancer

Presented by Babita Jyoti, MD (University of Florida)

Background: We present the trends in plasma pro-BNP and Troponin T levels recorded prospectively in breast cancer patients treated with proton therapy.

Methods: Eighteen patients treated with PT underwent a post-surgery, post-chemotherapy, pre-PT baseline and q3month post-PT biomarker evaluation including proBNP (normal range, 0-125 pg/mL) and troponin T levels on a prospective protocol. All patients required regional nodal irradiation. A dose of 50.4Gy(RBE) at 1.8Gy(RBE)/fraction was prescribed to the breast or chest wall and comprehensive regional lymphatics including IMN with a 10-16Gy(RBE) boost to the lumpectomy bed or mastectomy incision. PT was delivered using passive scattering alone or with photons. Cardiac DVH parameters were analyzed.

Results: The median patient age was 49.5 years (range, 37-73). Patient, diesease and treatment characteristics were as follows: 9 patients were African-American and 9 white; 9 had left- and 9 had right-sided cancers; 12 received anthracycline chemotherapy (3 trastuzumab), 5 received non-anthracycline chemotherapy (2 trastuzumab), and 1 received no chemotherapy. Pro-BNP remained <=125 in 9 patients (5 left-, 4 right-sided) while 9 experienced a rise >=125 (4 left-, 5 right-sided). Eight patients had a baseline >=125 (4 left-, 4 right-sided; 7 received anthracyclines, 1 received non-anthracycline chemotherapy). In 1 patient both markers rose at diagnosis of pulmonary embolism. The median follow-up for biomarkers was 16 months (range, 2 -36) with a trend to decline in median pro-BNP from preradiotherapy to last follow-up; all patients, 111.2 to 90.2; right side, 111.2 to 81.3; and left side, 102.8 to 90.9. Median troponin T showed no increase. Cardiac V5 (range, 0%-12.30%) and mean heart dose (range, 0-3.2 Gy) were recorded. Median mean heart dose was 0.5 Gy. There was no relationship between pro-BNP and cardiac dose.

Conclusion: Following systemic therapy and proton therapy for left- and right-sided breast cancer, median troponin T remained low while median pro-BNP was variable, with an overall decline from post-systemic therapy preradiotherapy baseline, suggesting that proton therapy did not result in cardiac injury measurable by troponin T or pro-BNP.

Proton lung treatments in the seated position: Development and installation of a vertically positioned CT scanner for imaging thorax patients

Presented by Draik Hecksel, PhD (Northwestern Medicine Chicago Proton Center)

The Northwestern Medicine Chicago Proton Center has two treatment rooms that utilize an incline gantry. The incline gantry system can couple the treatment nozzle to one of two fixed beam lines that enter the room at either 90 or 30 degrees for patient treatment. The use of two fixed beam lines with one moving nozzle reduces the size and cost of room construction while maintaining the ability to treat the majority of cases. However, the incline gantry design still has limited treatment geometry which disqualifies certain patients from those treatment rooms.

A novel system that includes a chair and vertically mounted CT scanner has been designed and installed in conjunction with P-Cure to enable imaging of patients in the seated position. Treatments in the seated position will permit the incline gantry room to use of a full range of anterior and posterior beam angles previously not available in the supine position. The new system is expected to increase the number patients that can be treated using the incline gantry and simultaneously reduce the number of patients requiring treatment utilizing the full 360? gantry.

The vertical CT scanner has been mounted to the ceiling and wall of an incline treatment room at a 70? tilt from the typical CT scanner orientation, which matches the angle of the chair back. The treatment

chair replaces the standard treatment couch on the robotic patient positioning system using a coupler mounted to the chair underneath the patient's thighs. For a CT scan, the robotic arm moves the patient to the CT isocenter. The CT scanner moves downwards from its parked position and performs the scan while the patient remains stationary. Multiple safety interlocks prevent the CT scanner from contacting the patient with excessive force.

Based on previous MRI based studies, we expect that treatment in a seated position may reduce the magnitude of tumor motion and increase lung volume. These two effects should decrease the radiation dose to healthy lung. Previous studies have also suggested that lung function is improved in the seated position.

Seamless spot-scanning proton beam therapy for unresectable, large (> 25 cm) soft tissue and bone sarcomas: two case reports

Presented by Takayuki Hashimoto, MD (Hokkaido University)

Proton beam therapy (PBT) provides dosimetric benefits over conformal x-ray therapy in sparing organs at risk when treating soft tissue and bone sarcoma because of the fundamental physical dose distribution of the proton beam. However, cases with extended lesions are difficult to treat using passive scattering system with a single isocentric field, as the length of the clinical target volume (CTV) is longer than the available PBT field size in many facilities. We report two cases of large (> 25 cm) soft tissue and bone sarcomas successfully treated by seamless spot-scanning PBT. Case 1: A 69-year-old man was diagnosed as stage III (UICC 7th) sacral chordoma (cT3N0M0). The primary tumor invaded the right gluteal muscles, and some daughter lesions were observed in the ileum, that was deemed unresectable. Maximum extent of the gross tumor volume (GTV) was 26 cm. He received PBT (CTV D99%=70 GyE in 28 fractions). No severe late toxicity has been observed. He developed multiple lung metastasis 1 year after PBT with local control. Case 2: A 55-year-old man was diagnosed as stage III (UICC 7th) liposarcoma (cT2bN0M0). A PET-CT scan showed the tumor located in inguinal region to retroperitoneal space, and maximum extent of the GTV was 26 cm. Surgical resection was considered to be impossible. He was considered stable disease and referred to our hospital after 3 months from 4 courses of chemotherapy (VAC: Vincristine, Actinomycin-D, Cyclophosphamide). The patient received PBT to a total dose of 70 GyE in 28 fractions (CTV D99%). A grade 1 skin reaction was observed during PBT, and no late toxicity of grade 3 or more was observed. Three months after PBT, his pain of iliac lesion was relieved. The patient has survived without recurrence nor metastasis for 6 months after PBT. Conclusion: Seamless spot-scanning PBT can be a useful treatment strategy for unresectable, large soft tissue and bone sarcomas.

Changes in Serum Testosterone 60 months after Proton Therapy for Localized Prostate Cancer

Presented by Romaine Charles Nichols Jr, MD (University of Florida)

Background: 5 studies in the contemporary radiotherapy literature have demonstrated a +/-10% decline in Serum Testosterone (ST) for patients receiving x-ray therapy for prostate cancer - presumably due to scatter radiation to the testicular Leydig cells.

Materials and Methods: Between August 2006 and October 2011, 399 patients with low and intermediate risk prostate cancer were enrolled on 3 prospective trials delivering between 70 Cobalt Gray Equivalent (CGE) and 82CGE at between 2CGE and 2.5CGE per fraction using passively

scattered protons. Serum testosterone (ST) was to be checked at baseline and every 6 months after PT. ST was checked at baseline in 393 patients and at 60 months or later in 169 of these patients (who are the subject for this analysis). The analysis excluded 14 patients who received LHRH agonist therapy before PT and 2 patients who acknowledged taking exogenous testosterone medications after PT.

Results: Median baseline ST for the analyzable patients was 374.4 ng/dl (range 120.1 to 791.0). Median ST 5 years after PT was 390.0 ng/dl (range 25.0 to 862.0). The difference was not statistically significant (p=0.9931).

Conclusion: Passively scattered proton therapy was not associated with testosterone suppression 5 years after PT - suggesting that protons may be associated with less out of field scatter radiation compared with x-rays.

Increasing Energy Layer Spacing in PBS plans to Reduce Beam Delivery Time while Maintaining Clinical Goals and Robustness

Presented by Hazel Ramirez (Northwestern Medicine Chicago Proton Center)

Objectives: Increasing the number of spots in a plan can potentially increase the beam-on time. In Pencil Beam Scanning (PBS), layer switching is another parameter which adds time. In RayStation, the Energy Layer Spacing parameter (ELS) is a value the planner can change to set the distance between layers. By increasing the ELS, we reduce the number of layers that cover the target. In this study we investigate the potential time savings translated to beam delivery with a larger layer spaced plan compared to the originally approved plan.

Methods: Breast, prostate, SFUD brain, MFO brain, and CSI plans were re-optimized in RayStation with increased ELS to achieve the same clinically defined objectives and robustness. At our center, layer switching can take 5-7 seconds. Spot scanning delivery within a layer can take 1-6 seconds depending on the number of spots. Beam delivery time was estimated by giving each layer a factor of 6 seconds and an additional 1 second was added for every 154 spots in the plan.

Results: The total number of layers used in a plan depends on target size. For targets at least 7cm wide an ELS of 1.3 can be used. For larger targets, it was possible to increase to 1.6. There was no significant time savings when just 1 layer was removed. This was due to the optimizer adding more spots into the plan to achieve the same clinical objectives. Starting with ELS of 1.3 an average time savings of 53-138 seconds per field was observed for each breast and CSI plan with the removal of 12-22 layers for breast and 7-16 layers for CSI. For prostate and SFUD brain up to 7-8 layers could be removed for a max savings of 45 seconds per field. MFO brain saved an average of 30-66 seconds per field with the removal of 6-12 layers.

Conclusions: It is possible to decrease the number of layers and spots to decrease delivery time and still maintain a clinically acceptable and robust plan. The ELS value is target size dependent. Because of this it is not recommended to have constant ELS. Decreasing delivery time can increase efficiency by increasing throughput which adds timeslots for more patients or QA, reducing wait time in queue, and reducing the potential for beam pausing. In addition, decreasing time can potentially reduce intra-

fraction uncertainties from patient motion, time for volumetric repainting, and patient anxiety from prolonged treatment.

Low Acute Symptom Burden of Proton Beam Therapy for Primary Brain Tumors

Presented by J. Ben Wilkinson, MD (Willis-Knighton Cancer Center)

Purpose: To determine acute toxicity profile for patients treated with definitive proton beam therapy (PBT) for primary brain tumors at a single institution using pencil beam scanning (PBT) and cone-beam CT (CBCT) image guidance.

Methods: A prospective, IRB-approved PBT registry was queried to identify patients who were treated for a primary brain tumor between September 2014 and April 2016. Patients were required to have completed toxicity profiles at baseline, end of treatment, and three months for inclusion in this analysis. Incidence and change in grade of toxicities at baseline, end of treatment, and three-month follow-up was calculated for each patient. Toxicities were assessed using the CTCAE version 4.0 and the SALT (Severity of Alopecia Tool) score for alopecia.

Results: Out of 32 patients treated with PBT for CNS disease, 20 patients met study entry criteria and were analyzed. Average age was 59.5 years with 60% being female and an average Zubrod score of 0.6 at baseline. Tumor pathology was predominantly glioma (80%) and high grade (87%). Other histologies included meningiomas (n=2), chordomas (n=1), and hemangioblastomas (n=1). Alopecia was the only statistically significant change in toxicity with SALT score decreasing from an average baseline score of 98 to end of treatment 76.6 + 16.2 ($p<0.001$) with modest recovery at 3-month follow-up up to 84.5 + 10.4 ($p=0.01$). Headaches were common before and after treatment with average grade maintained at 0.6 + 0.5. Motor neuropathy showed a non-significant increase going from 0.3 + 0.7 to 0.6 + 1.0 to 0.6 + 1.0 (baseline, end of treatment, 3 month follow up; respectively). Ataxia also showed a non-s ignificant increase going from 0.3 + 0.6 to 0.4 + 0.8 to 0.5 + 1.0. All other toxicities had an average grade less than 0.2 at any time point including nausea, vomiting, fatigue, amnesia, and sensory neuropathy. There were no acute grade 3 toxicities experienced by this cohort.

Conclusions: Proton beam therapy produces low levels of acute treatment-related toxicity for brain irradiation with alopecia being the only statistically significant symptom change in this study. Larger studies are needed to determine if other clinically meaningful, treatment-related toxicities exist.

Proton beam therapy for pediatric patients with rhabdomyosarcoma. A Japanese national survey

Presented by Masashi Mizumoto, MD, PhD (University of Tsukuba)

Purpose: To evaluate efficacy of proton beam therapy (PBT) for pediatric patients with rhabdomyosarcoma in Japan.

Materials and Methods: From 1987 to 2014, PBT was conducted in 71 patients with rhabdomyosarcoma at three institutes in Japan. The patients group consisted of 44 boys and 27 girls, and the age ranged from 0 to 19 (median 5) years old. The tumor location were head and neck, urinary organ, parameningeal, retroperitoneal and others 37, 12, 11, 4 and 7, respectively. Pathologic subtypes were embryonal rhabdomyosarcoma (n=39), alveolar rhabdomyosarcoma (n=27) and other rabdomyosarcoma (n=5), respectively. 56 patients received PBT as an initial treatment and 15 received PBT for

recurrence cases. According to COG classifications 9, 38 and 9 were classified into low, intermediate and high risk group, respectively. The given doses were ranged 18.0 to 60.0 GyE (median 50.4 GyE).

Results: The overall survival rates after 1 and 3 years were 90% and 83%, 65% and 45% for initial treatment case and recurrence cases, respectively. According to COG classifications 1 and 3 year survival rate were 100% and 100%, 94% and 90%, 67% and 15% for low risk, intermediate risk and high risk group, respectively. Median follow-up period for survivor was 26 months. 9 of 56 patients had Grade 2 late toxicity and Grade 3 or more late toxicity was not observed. Two second malignancy was observed after PBT. One was myelodysplastic syndrome and the other was osteosarcoma occurred outside the irradiated field.

Conclusion: This study provides preliminary results of PBT for rhabdomyosarcoma in Japan. More experience and follow-up with this technique are required to establish the efficacy of PBT.

Incidence of Brainstem Necrosis Following Proton Therapy for Posterior Fossa Tumors in Children

Presented by Daniel Indelicato, MD (University of Florida)

Background: Contemporary single institution data suggests that the rate of CNS necrosis in pediatric patients with posterior fossa tumors following 54 Gy photon radiation is approximately 4.4% (Murphy, 2012). The purpose of this study is to estimate the risk of CNS necrosis in a similar cohort treated with proton therapy.

Methods: Between 2007-2016, 225 children <=21 years old with posterior fossa ependymoma (n = 101), medulloblastoma (n = 77), glioma (n= 33), ATRT (n = 12), and meningioma (n = 2) were treated at a single institution with double-scattered proton therapy. The median follow-up was 3.0 years (0.2-8.8 years). The median prescribed dose for the whole cohort was 55.1 GyRBE. Brainstem necrosis was defined as new or progressive symptoms involving motor weakness or cranial nerves V-VII or IX-XII with a corresponding radiographic abnormality within the brainstem in the absence of disease progression. Toxicity was graded according to modified CTCAE criteria.

Results: The 3 year actuarial rate of brainstem necrosis was 4.9%. The rates of grade 3+ and grade 5 necrosis were 1.7% and 0.8%, respectively. Brainstem necrosis was identified between 3-12 months following radiation. For the patients who experienced necrosis, the median prescribed dose, brainstem D50%, brainstem D10%, and brainstem maximum 0.1 cc dose was 55.5 GyRBE, 55.1 GyRBE, 57 GyRBE, and 57.8 GyRBE, respectively. For patients who did not experience necrosis, the median prescribed dose, brainstem D50%, brainstem D10%, and brainstem maximum 0.1 cc dose were 55.1 GyRBE, 48.1 GyRBE, 54.3 GyRBE, and 55.7 GyRBE, respectively. All living patients have recovered with a KPS >70%.

Conclusions: The incidence and severity of brainstem necrosis following double-scattered proton therapy in children with posterior fossa tumors seems to be comparable to photon experiences. This data is critical in guiding treatment of tumors where the brainstem is within the PTV.

Long-term follow-up after proton beam therapy for pediatric tumors: A single institute experience

Presented by Yoshiko Oshiro, MD (University of Tsukuba)

Objective: Proton beam therapy is expected as a new treatment option in place of traditional photon radiotherapy that may reduce the risk of late toxicity and secondary cancer, especially for pediatric tumors. The goal of this study was to evaluate the long-term benefits of PBT in cancer survivors.

Methods: A retrospective observational study of pediatric patients who received PBT was performed at one institute. From 1984 to 2014, 225 pediatric patients received PBT at our institute. Of 225 patients, 37 were followed up for 5 or more years. These patients included 22 males and 15 females, and had a median age of 10 years (range: 0-19 years) at the time of PBT. The irradiation dose ranged from 10.8 to 70.2 GyE (median: 41.4 GyE). The tumor types were rhabdomyosarcoma, arteriovenous malformation (AVM), brain tumor, head and neck tumor, neuroblastoma, skull base tumor, Ewing sarcoma and others in 9, 7, 5, 4, 4, 2, 1 and 5 patients, respectively. The median follow-up period was 9.4 years (5.0-31.2 years).

Results: 12 of 37 patients had grade 2 or more late toxicities. 5 of 12 events were facial deformity, 2 were growth hormone deficiency. The 5-, 10- and 20-year rates for grade 2 or higher late toxicities were 11%, 28% and 39%, respectively, and those for grade 3 or higher late toxicities were 3%, 10% and 10% respectively. No secondary malignant tumors occurred within the irradiated field. One patients had pituitary adenoid within the irradiated field 8 years after PBT.

Conclusion: Deformity cannot be avoided within the treatment field, but rate of other late morbidities including secondary malignancy was low by using PBT. Further follow-up is needed to confirm the benefits of PBT for pediatric tumors.

A dosimetric comparison of helical tomotherapy and intensity modulated proton therapy for selected pediatric cases

Presented by Elisa Coassin, MD (University of Milan)

Objectives: To evaluate the performance of helical tomotherapy (HT) and intensity modulated proton therapy (IMPT) on a group of complex pediatric cases..

Methods: Eighteen patients (age 2.5-19.5) treated at a curative intent with HT were re-planned for IMPT. Tumor types: orbital, parameningeal, bladder/prostate rhabdomyosarcoma; cervical-thoracic chordoma; paravertebral, sacral, pleural Ewing's sarcoma; tibial Ewing's sarcoma with primary bone metastases; incompletely resected posterior fossa ependymoma; craniopharyngioma; atypical teratoid/rhabdoid tumor of the quadrigeminal/pineal region; papillary tumor of the pineal region; standard-risk medulloblastoma; lacrimal gland incompletely resected adenoid cystic carcinoma; nasopharyngeal carcinoma; esophageal cancer (second malignancy 7 years after thoracic HT); supradiaphragmatic and supra/infradiaphragmatic Hodgkin's disease. Treatment sites: head and neck (n=4), brain (n=4), thorax (n=4), pelvis (n=3), spine (n=2), craniospinal (n=1). Prescribed doses: 14.4-67.4 Gy. Five cases were planned using a simultaneous integrated boost strategy (in one patient as part of total pleural irradiation). Spinal cases were planned with a simultaneous integrated dose reduction approach. In one case a high-dose stereotactic boost partially involving the brainstem followed the first phase of treatment. A simultaneous treatment of multiple sites was included. A dosimetric comparison evaluating target coverage (D2, D98), homogeneity (D2-D98), conformity (CI95) and organs at risk (OARs) sparing (DVH constraints meeting for selected OARs) between HT and IMPT was performed. In order to make a fair comparison in terms of OARs sparing, proton plans aimed at a homogeneous coverage of HT PTVs.

Results: The median number of beams used for re-planning was 3 (1-6). Thirty-six PTVs were evaluated. IMPT increased adherence to the prescribed PTV minimum and maximum dose by 1.2% and 0.1%, respectively. D98 improved in 60% of PTVs; D2 in 58.6% of PTVs. IMPT was superior in terms of homogeneity in 68.4% of PTVs and conformity in 70.6% of PTVs. Constraints were met for 87.5% of OARs with HT (33.3-100%), and for 91.7% (75-100%) with IMPT. IMPT further enhanced DVHs for 72.5% of met and for 83.3% of unmet OARs constraints (median reduction factor below the constraint 1.4 and 1.2, respectively), with the main advantages resulting in: heart sparing in total pleural irradiation, contralateral OARs sparing in one-sided head and neck treatments, cochlea sparing in posterior fossa treatment.

Conclusions: IMPT demonstrated superior target coverage, homogeneity, conformity, and OARs sparing. The greatest benefit of IMPT was seen in brain and pelvic tumors. In orbital rhabdomyosarcoma, HT was shown to be superior, thanks to the sharper penumbra of photon beams at shallow depths.

QMRI Analysis of PRT-Induced Structural Changes in Pediatric Medulloblastoma Survivors: Potential Predictor of Neurocognitive Trajectory

Presented by Andrew Zureick, BS (Harvard University)

Background: Proton radiotherapy (PRT) helps to mitigate the adverse neurocognitive effects of radiotherapy in pediatric medulloblastoma patients. Here, we employ quantitative MRI analysis to investigate the relationship between PRT-induced structural changes in the brain and neurocognitive late effects, using full-scale IQ (FSIQ) and its four component indices: verbal comprehension (VCI), perceptual reasoning (PRI), working memory (WM), and processing speed (PS).

Methods: 18 pediatric medulloblastoma patients (median age at PRT = 6.9, range 3.6-20.1) treated with CSI PRT were identified via the Phase II study NCT00105560 (Yock et al., Lancet Oncology 2016), with routine surveillance imaging studies and baseline/follow-up neurocognitive evaluations available. T1 MRI images were converted to NIFTI format and underwent bias correction, skull stripping, and atlas-based autosegmentation into 83 regions-of-interest (ROI). Univariate and multivariate linear regression was performed to investigate how 85 variables (age, gender, and all ROI volumes), alone and in subsets, best correlate in models to predict neurocognitive scores.

Results: Median neurocognitive follow-up was 2.4 years (range 1.5 - 6.5 years). In univariate analysis, no single ROI consistently correlated with all neurocognitive measures, though each measure had individually highly-correlated ROI volumes. In multivariate feature selection, higher VCI scores were best predicted by older age and larger left hippocampus (LHC), right hippocampus (RHC), and left amygdala (LA) volumes, taken together (leave-one-out cross-validation error [LOO-CVError] = 0.527 points). Higher PRI scores were best predicted by older age and larger LHC, RHC, and LA volumes (LOO-CVError = 2.68 points). Higher PS scores were best predicted by older age and larger LHC and RHC volumes (LOO-CVError = 0.957 points). Higher FSIQ scores were best predicted by right anterior cingulate gyrus (smaller), right pre-subgenual frontal cortex (larger), left lateral remainder of the occipital lobe (larger), and left nucleus accumbens (larger) volumes (LOO-CVError = 1.31 points) . Insufficient neurocognitive data was available for analysis of WM scores. Results for a larger cohort will be presented.

Conclusions: Our preliminary analysis showed a consistent relationship of older age and larger hippocampal volumes with higher neurocognitive scores. Future work will involve longitudinal analysis

with a temporal component, features such as regional ADC and surface measurements, and inclusion of age- and gender-matched controls.

Effects of Vertebral Body Sparing Proton Craniospinal Irradiation on the Spine of Young Pediatric Patients with Medulloblastoma

Presented by Brian Chou (Loma Linda University Medical Center)

Introduction: Proton therapy is widely accepted in the treatment of pediatric malignancies, including craniospinal irradiation (CSI) for medulloblastoma. Common practice for proton CSI has been to include the entire vertebral body of growing patients in the clinical target volume in an effort to minimize asymmetrical bone growth, which is thought to cause spinal deformities such as scoliosis or lordosis. However, data suggests scoliosis rates remain high despite treatment of the entire vertebral body. This retrospective case series investigates the suitability and long-term effects of vertebral body sparing proton CSI on the spine of young patients.

Materials and Methods: Six children between the ages of 3 and 5 years with medulloblastoma were treated with vertebral body sparing CSI. Each patient received maximal safe resection prior to radiation treatment. Radiation therapy was delivered in the supine position with posterior beams targeting the craniospinal axis, and the proton beam was stopped anterior to the thecal sac. Based on risk stratification and investigational protocols, patients were treated with either a dose of 23.4 or 36 Colbalt Gray Equivalent (CGE) to the craniospinal axis followed by a proton boost to the posterior fossa. Chemotherapy varied by protocol. Radiographic effects on the spine were evaluated with serial imaging, either with MRI or plain film using Cobb angle calculations, the presence of thoracic lordosis, lumbar vertebral body-to-disc height ratios, and anterior-posterior height ratios. Clinical outcomes were evaluated by patient/family interview and medical chart review.

Results: Five of six children were alive at the time of follow-up. Overall survival was 83% (5/6) and disease free survival was 100% (6/6). Median clinical and radiographic follow-up were 13.6 and 12.3 years, respectively. Two patients have been clinically diagnosed with scoliosis and have been treated conservatively. At the time of follow-up, no patients have suffered chronic back pain or required spine surgery. No patients were identified to have thoracic lordosis. Diminished growth of the posterior portions of vertebral bodies was identified in all patients with an average posterior to anterior ratio (PAR) of 0.88, which was accompanied by compensatory hypertrophy of the posterior intervertebral discs.

Conclusion: Vertebral body sparing CSI with proton beam did not cause severe spinal abnormalities in the patients treated at our institution. This approach could be considered in future clinical trials in an effort to reduce toxicity, risk of secondary malignancy, and preserve adult height.

Comparison of hydrogel spacer and rectal immobilization on intra-fraction motion equivalence using image guidance prostate proton therapy

Presented by Alfredo Mirandola, PhD (Fondazione CNAO)

A modular multilayer ionization chamber for hadron beam intensity, spot position and profiles evaluation was tested at the Centro Nazionale Adronterapia Oncologica (CNAO), a synchrotron-based proton and carbon ion facility in Pavia (Italy).

QUBE includes a stack of integral ionization chambers (MLIC-module) with a 1 mm air gap to instantaneously evaluate the particle beams depth-dose distributions at different energies and modulations (SOBP and pristine Bragg Peaks) with a water equivalent resolution of ~2.34 mm and up to a maximum range of ~300 mm. The depth-dose distribution curves of both proton and carbon ion beams were acquired and compared with the measurements performed with PTW Peakfinder. The gain calibration factors of each channel are energy and particle independent and were obtained by irradiating the device at maximum energy from both sides. They are all within 20%. The repeatability in the Bragg Peak position estimation was tested by delivering 10 consecutive spills for each tested energy showing standard deviations < 1 % for both protons and carbon ions. The accuracy in range evaluation, assessed by delivering a 150 MeV/u carbon ion beam and putting 5 PMMA slabs of decreasing thickness (from 1 down to 0.2 mm) in front of the device, resulted to be about 0.3 mm. QUBE also includes a STRIP-module for the evaluation of the beam profile and position along X and Y directions with sensitive area of 12.7x12.7 cm2, an air gap of 2 mm and a native strip spatial resolution of 1 mm. The spot center of gravity (CoG) was computed as weighted sum of the counts in the strips, in both X and Y directions. The maximum displacement in the beam CoG estimation was <0.1 mm. Spot size was measured with the STRIP-module and compared with the data acquired with the radiochromic EBT3 films. The device showed optimal performances with both proton and carbon ion beams and can be used to speed up Quality Assurance procedures in clinical facilities.

Small Field Proton Radiosurgery Using the Plateau Region of the Depth Dose Curve

Presented by Michael Lamba, PhD (University of Cincinnati)

Introduction: Proton therapy produces advantageous dose distributions relative to other types of radiation. However, for very small fields the Bragg peak can be significantly reduced, even falling below the plateau region. Additionally, uncertainties in the depth of the Bragg peak result in plans with extra treatment margins. Proton radiation in the plateau region of the depth dose curve has physical characteristics that may be advantageous relative to photon radiation for application in radiosurgery treatments. Primary among these is the relatively low secondary electron energy, with a maximum of approximately 500 keV. Secondary electrons play a significant role in the penumbra of small collimated proton beams. Proton therapy with targets at the plateau region was employed in early proton therapy, in which 340 MeV proton beams were used to treat pituitary tumors with multiple non-coplanar image-guided beams.

Methods: This study simulated aperture-shaped high energy proton beams modeled in a radiosurgery treatment planning system and compared the results to a clinical photon plan. Monte Carlo simulation (Topas v1.0) was performed to generate a parallel source of 200MeV protons incident on a cylindrical water phantom of diameter 20.0 cm and depth of 20.0 cm. An 8.0 cm thick brass collimator with a 4.0 mm aperture was placed at a distance of 6 cm from the phantom surface. A cross-profile for the collimated proton field at 5 cm depth in the phantom was created after scoring 18 million particle histories. The cross profile and depth dose were modeled in the radiosurgery planning system (Brainlab Brainscan). CT and thin-cut MR were imported, fused, and the left trigeminal nerved identified as a target. Treatment plans consisting of 15 arcs were generated for both the simulated 4 mm proton and clinical 4 mm photon beams treating to 80 Gy maximum dose to the nerve.

Results: The maximum doses to the brainstem were 12.8 Gy and 19.2 Gy for the proton and photon plans, respectively. The proton/photon ratio of the dose volumes ranged from approximately 1 at 70 Gy to 0.5 at 10 Gy.

Conclusions: While significant further validation is necessary, proton radiosurgery using the plateau region of the depth dose curve may hold promise for improved dose distributions and critical structure sparing over photon radiosurgery for very small fields.

Fast Monolithic System for Proton Imaging

Presented by Fritz DeJongh, PhD (ProtonVDA, Inc)

Purpose: Proton radiography would be the most direct method of image guidance for proton therapy. There is a need to enable more complex treatments delivering a high dose to the tumor with reduced uncertainty. There is also a need to maintain patient throughput and improve the cost-effectiveness of proton therapy relative to conventional radiation therapy. The use of a proton beam for both imaging and treatment streamlines patient setup and quality assurance procedures, reduces alignment uncertainties, and reduces proton range uncertainties. We aimed to develop a high-performance, low-cost proton radiography system based on well-established fast scintillator technology.

Methodology: We established the feasibility for both a residual range detector and a tracking detector. The design of our system is based on requirements that the final clinical detector system be:

Simple and lightweight.

Easily scaled to large field sizes.

Capable of operating at high speed to maximize patient throughput.

Expose the patient to the minimum possible radiation dose for a given resolution.

Our specific aims were to construct and test a prototype high-speed residual range detector and a prototype tracking detector..

Conclusion: The combination of high performance, simple monolithic construction and reduced electronics channel count will enable us to develop a clinically practical system.

Evaluating the Dose and Image Quality of Proton Computed Tomography using a Filtered Backprojection Reconstruction from Monte-Carlo Cone-Beam Projection Simulations

Presented by Derek Moyer, MS (University of Cincinnati)

Introduction: Photon computed tomography includes an uncertainty in the prediction of a protons range that can be as large as 3.5% which can have significant effects on the quality and robustness of proton plans. A CT using a proton source (PCT) is a more direct measurement of stopping power. This Monte Carlo study evaluates the image dose and image quality of PCT.

Materials and Methods: TOPaS, a Monte Carlo platform, was used to simulate a cone beam source of protons traversing though a 16 cm sphere water phantom containing six spheres made of bone, lung,

adipose tissue, and muscle. Ten million 250 MeV proton particles were simulated for 180 projections, each separated by two degrees. Monte Carlo tabulated proton tracks and proton energy at a detector plane were imported into Matlab to create energy projection images. Two methods of creating projection images were used, an energy sum and an energy integral. The energy sum was a summation of all protons energy at the detector, while the energy integral process used calculated values for each proton based upon the energy specific stopping power at different points along a protons path. A pre-weighting function was then applied to minimize the contribution of protons near the periphery of the cone beam. The Open Source Cone-beam Reconstruction code (OSCaR) was used to filter and backproject the weighted projection data. The contrast-to-noise ratio(CNR) and dose to various parts of the reconstructed phantom were evaluated..

Results: The dose from 1.8x109 protons projected onto a 16 cm sphere ranged from 5.4-7.9mGy. CNRs of 9.94 and 7.75 were observed for the bone sphere from the energy sum and energy integral backprojections respectively. The contrast was insufficient to detect other materials.

Conclusion: PCT at the simulated number of protons produces insufficient signal-to-noise to improve stopping power uncertainty. Increasing the number of protons, and therefore dose, to levels comparable to, or above, those of conventional CT may improve signal-to-noise (SNR) sufficiently to for stopping power uncertainty reduction. Continued investigations of interest include effects on image reconstruction from multiple small angle proton scatter, and clinical goals for CNR, SNR and spatial resolution.

Analyzing the effect of range shifter thickness and air gap on TPS dose modeling accuracy in superficial PBS proton therapy

Presented by Robert Shirey, MS (Willis-Knighton Cancer Center)

Purpose: Treatment planning systems (TPS) using pencil beam dose algorithms do not accurately model superficial dose distributions of range shifted proton pencil beam scanning (PBS) treatments. Though most commercially available proton TPS use a PB dose algorithm, no studies could be found which quantify the functional dependence of TPS dose error on depth or air gap. This study quantifies dose error from the RayStation5 PB dose algorithm as a function of range shifter (RS) air gap and treatment depth for superficial proton PBS treatments using two range shifters of different thickness.

Methods: Using Raystation5, fourteen treatment plans with varying air gaps were created for each RS. Line dose profiles determined the TPS doses at varying depths from the surface to 5 cm. An IBA ProteusONE system with 3.5 and 6.5 cm Lucite range shifters delivered the treatment plans. An IBA-Dosimetry PPC05 ion chamber measured dose at ten depths within the RW3 water-equivalent phantom. Water-equivalent thickness of the chamber window was calculated and accounted for. Measured dose was corrected for daily beam output variations.

Results: TPS dose error has a dependence on both depth and air gap. TPS error decreases as depth increases and as air gap decreases. At depths <1 cm, the 3.5 cm RS has an average dose error of 1.4%, 2.8%, 5.4%, and 7.7% at air gaps <5 cm, 5-10 cm, 10-20 cm, and >20 cm, respectively. At depths >1 cm, the corresponding dose errors are 0.9%, 2.2%, 3.4%, and 5.0%. The dose error of the 6.5 cm RS increased, on average, by a factor of 1.5.

Conclusions: For the first time, this study comprehensively quantifies TPS dose error of range-shifted proton fields as a function of depth, air gap, and RS thickness. When PB dose algorithms are used to create superficial PBS treatments, a thinner RS should be used and the air gap should be kept less than 10 cm when patient setup allows. Poor modeling of secondary proton scatter generated in the RS (nuclear halo effect) is the main contributor to TPS dose overestimate. Future implementation of a Monte Carlo dose engine should eliminate this error. A continuation of this research will determine the dose error from the Monte Carlo dose engine in RayStation6.

The Reconstruction of the Four-Dimensional Dose Distribution in Spot-Scanning Proton Beam Therapy Using the Fiducial Marker Motion and Treatment Machine Log Data

Presented by Shusuke Hirayama, PhD (Hokkaido University)

Purpose: Real-time image-gated proton beam therapy (RGPT) system has been developed and clinically used for moving tumors. In this system, two fluoroscopic images of the gold sphere fiducial marker (1.5-2.0 mm in diameter), which is inserted near the tumor in a patient, are monitored in real-time, and the scanned proton beam is gated when the marker enters within the pre-assigned gating window (GW) set ? 2 mm around the planned positions. In this work, we describe a system design to reconstruct the dose distributions delivered to patients through the course of the RGPT.

Materials and Methods: The system uses the RT Plan data and planning CT images exported from the treatment planning system, and three separate log data: (1) the three-dimensional trajectory of a fiducial marker recorded by the RGPT system, (2) treatment log data exported from the treatment control system which is comprised of the positions and monitor unit (MU) values for all delivered spots, and (3) the timing data of each spot beam delivery and pulsed X-ray exposure signal recorded by the in-house signal analyzing system. The log data were synchronized to derive the modified spot files, which include both the effect of patient motion and the uncertainty in spot positions and MU values. The actual dose distribution was calculated using pencil beam algorithm on the basis of the modified spot files.

Results: Among the synchronized log data, the energy levels, number of spots, and the gate signal shapes were shown to be consistent. Using the modified spot files, the dose distribution was successfully calculated.

Conclusions: We designed the four-dimensional dose reconstruction system using the fiducial marker motion data and the treatment log data obtained during the RGPT. It was shown that the system can potentially evaluate the interplay effect accurately for patients receiving the RGPT.

Poster Abstracts

Accuracy Map of a Robotic Patient Positioning System Equipped with an Integrated Optical Tracking System

Presented by Alexander Ableitinger, MSc (EBG MedAustron Gmbh)

Introduction: Clinically employed robotic patient positioning systems (PPS) must consider weight-induced couch bending to achieve the required positioning accuracy. Exact localization of the patient's center of mass and weight is therefore for these robotic systems crucial.

The PPS at MedAustron overcomes the use of cumbersome look-up tables by employing a photogrammetric camera. The treatment couch is tracked and an iterative position correction loop aligns the couch. Aim of the current work is to determine the positioning accuracy of this new technology.

Material and Methods: A lasertracker was used as the reference instrument in the validation of the correct couch position. The treatment volume has a dimension of 115 cm x 50 cm x 40 cm on the treatment couch. The robotic system enables couch rotations of 190 °, pitch and roll of +/- 3 ° and non-isocentric treatment positions. The spatial deviations for 6120 measurement points localized and corrected with camera system and determined with lasertracker were investigated for 1020 different robot positions, poses and payloads.

Results: The differences between prescribed and measured position for all measurement points were statistically evaluated in terms of axis specific histograms and their overall 3D deviation. For 95% of all measurement points the 3D accuracy was better than 0.63 mm. The mean deviations of the individual coordinates were in x:0.24 mm, y: -0.02 mm and z: -0,22 mm. Regarding the weight-induced couch bending no correlation of the accuracy and the payload could be detected.

Conclusion: These results show that mass-induced flex of the couch can be automatically compensated by a tracking-based feedback loop providing high level of accuracy in patient positioning.

Feasibility of Complex Chestwall Treatment with Pencil Beam Proton Therapy: A Case Series

Presented by Safia Ahmed, MD (Mayo Clinic)

Purpose: Complex chestwall tumors (e.g., thoracic sarcomas) present a challenge for radiation planning in terms of adequate target coverage with high doses and minimization of dose to avoidance structures. The feasibility of proton therapy for these cases is not reported. We present the first clinical application of pencil beam proton therapy for complex chestwall treatments.

Methods: Three patients received proton therapy as a component of their thoracic radiation treatment. Dose was prescribed such that >95% of CTV received ≥95% of prescription dose, while maximally sparing cardiac, pulmonary, and esophageal structures. Multiple anterior and posterior fields were utilized and spaced for skin-sparing. Plans with 10 mm spot spacing intervals were generated for an average in-air sigma of 10 mm, with energy layer-based repainting. Weekly CT verification scans were obtained until patient anatomy and dose consistently matched the original plan. New plans were created if verification scan(s) demonstrated anatomic and/or dosimetric changes.

Results: Histologies and associated tumor sites included mediastinal and right chestwall alveolar rhabdomyosarcoma with bilateral pulmonary nodules (patient #1); right hilar recurrent alveolar rhabdomyosarcoma with right lung and pleural nodules (patient #2); and right chestwall Ewing sarcoma with mediastinal, right internal mammary, and pleural metastases (patient #3). Patient #3 also had a contralateral chestwall internal cardiac defibrillator. Patients #1 and #2 received 15 Gy whole-lung photon radiation followed by a 36 Gy proton boost. Patient #3 received 15 Gy whole-lung proton radiation followed by a 39.6 Gy proton boost. Sum plans were available for patients #2 and #3. For patient #3, 86.3% of the sum prescription dose covered >=95% of the CTV. All other plans achieved >=95% coverage of CTV. Mean heart, contralateral lung, and esophagus doses were less than 22.5 Gy, 5.4 Gy, and 35 Gy, respectively, for the sum plans. Contralateral lung V20Gy was less than 5.4 Gy. Mean heart, contralateral lung, and esophagus doses were 11.7 Gy, 4.7 Gy, and 11.1 Gy, respectively, for patient #1's boost plan. The number of verification scans and re-plans were: patient #1, three scans and no re-plans; patient #2, one scan and no re-plans; patient #3, six scans and 10 re-plans.

Conclusions: Pencil beam proton therapy is feasible and enables delivery of high radiation doses to complex chestwall tumors with acceptable coverage and improved sparing of surrounding normal structures. Optimal planning for these cases is labor intensive, requiring CT verification scans and re-planning if necessary.

An Extensive Analysis of Clinical Trials Involving Proton Beam Therapy over the Past 20 Years

Presented by Jonathan B. Ashman, MD, PhD (Mayo Clinic)

Purpose: Proton Beam Therapy (PBT) is a rapidly growing radiation treatment modality. Conducting PBT clinical trials (CTs) are important in determining the benefits available through PBT in cancer treatments. An analysis of PBT trials is thus warranted to understand the current state of PBT CTs, and the factors affecting current and future trials.

Methods and Materials: We queried the clinicaltrials.gov website using the search terms: Proton Beam Therapy, Proton Radiation, and Protons. Exclusion terms were used to ensure that the search results were limited to CTs involving radiation therapy utilization, and, specifically, PBT. A total of 152 PBT CTs were identified. Characteristics of individual CTs were obtained. Chi-square analysis and logistic regression were used to evaluate trial characteristics.

Results: The majority of the CTs were active and recruiting (51.9%), phase II (62.5%), involving adults only (82%), located in the United States (86.1%), open label (88.1%), single group assignment (55.2%), and with a primary treatment endpoint of safety and efficacy (61.8%). The primary treatment sites included gastrointestinal (21.1%), central nervous system (20.4%), lung (13.8%), prostate (12.5%), sarcoma (9.9%), and others (15.7%). Comparison studies between radiation modalities involved PBT and

IMRT (7.2%), PBT and general photon therapy (5.2%), and PBT and carbon ion therapy (4.6%). PBT CTs underwent substantial growth post 2008, but now appear to be in decline. Non-governmental institutions (NGIs), comprising of university centers, hospital systems, and research groups, have funded the greatest number of CTs (69.7%). The NIH was more likely to fund CTs involving the CNS (p=0.02). Trials involving NIH funding were more likely to result in successful trial completion (p=0.02).

Conclusion: There has been a moderate amount of PBT CTs over the past 20 years focusing on diverse treatment sites. Among these, phase II trials have been the majority, with a very small minority being phase III CTs. We also noted limited funding of PBT CTs originating from industry or the NIH. Recently, there has been a declining trajectory of newly initiated PBT trials. With a growing number of PBT centers both in the United States and worldwide as well as increasing pressure to generate evidence justifying the clinical benefits of PBT, it is not yet clear whether this represents a true trend or just a pause in CT implementation. Despite multiple impediments to PBT CTs, the particle therapy community continues to work toward evidence generation.

Estimating Carbon Ion Radiation Therapy Interfractional Motion Error and Comparison with Normal Distributions

Presented by Daniel Bridges, BS, MMP (Gunma University Heavy Ion Medical Center)

Introduction: Prostate carbon ion radiation therapy (CIRT) has excellent local control and low toxicity. Given the prevalence of IGRT, it is concerning that the Gunma University Heavy Ion Medical Center (GHMC) uses only two-dimensional bone-matching for patient positioning. To clarify clinical acceptability, we investigate the acceptability of CTV and PTV margins as a function of interfractional motion. We also consider using Bayesian statistics for adaptive radiotherapy, given earlier literature recommending assumption of normal distributions.

Materials and Methods: At Gunma University Hospital (GUH) patients are supine with leg immobilization, CBCT images are acquired, the CBCT is automatically rigidly registered to the planning CT via bony anatomy, and the technologist shifts the patient couch to match prostate position by visual comparison with the planning CT. 1731 of these table shifts from 89 IMXT prostate patients were exported from Elekta Volume View. A prostate CIRT patient's DICOM files were exported from XiO-N 4.47 and MIM 6.5 at the GHMC to MATLAB R2016a. Target definitions: CTV = Prostate + Seminal Vesicles (SV). PTV1 = CTV + 10 mm (around Prostate) – 5 mm (Posterior) – 4 mm (Superior+Inferior) + (around SV)(5 mm uniformly – 2 mm Left+Right). PTV2 = PTV1 – rectum using flat cutline – 6 mm (Superior+Inferior). An IMXT-table-shift-weighted arithmetic average of the carbon dose was generated in MATLAB: This dose was written to a DICOM file, imported in MIM and VelocityAI for visual and DVH analysis. MATLAB was the n used to evaluate whether the shifts were characterized by normal distributions via cumulative distribution probability plot and 3D normal function comparison.

Results and Discussion: The averaged dose is less than planned for the rectum, although greater for the bladder, e.g., 9% more volume receiving 20 Gy (RBE). This dose-shifting method neglects stopping power changes in soft tissue (i.e., no organ deformation) and assumes that biological response can be averaged like dose. Dose streaking border artifacts are seen from shifting the entire dose. Neglecting deformation of rectum, bladder, and seminal vesicles may be a significant shortcoming. Shifts were not normal distributions either in independent axes or in 3D as seen clinically, as expected given specialized anatomical structure.

Conclusion: Assuming no organ deformation, 2D AP-and-lateral bone-matching with our planning target margins ensure planned dose to the CTV of prostate CIRT patients while sparing the anterior rectal wall. Normal distributions should not be assumed to use Bayesian statistics for interfractional motion prediction.

Is There a Quality Assurance Metric that can be Used to Screen for Contour Inaccuracies Prior to Radiation Therapy for Prostate Cancer?

Presented by Curtis Bryant, MD, MPH (University of Florida)

Objective: Assuring contour accuracy of treatment volumes before radiation therapy delivery is a major challenge for quality assurance teams at high-volume radiation therapy centers. Patients with contours that are drawn inaccurately may be at higher risk for disease recurrence after radiation therapy. For patients with prostate cancer, the prostate ultrasound volume attained at the time of biopsy may help to estimate contour accuracy before treatment delivery. The purpose of this study was to evaluate the prostate-target-volume-to-prostate-ultrasound-volume (PrTV/PUV) ratio and its association with contour accuracy for patients treated with proton therapy for prostate cancer. The second objective was to determine if contouring errors are associated with biochemical failure after proton therapy.

Materials and Methods: A matched-pair analysis was performed that included 45 men treated with proton therapy for intermediate-risk prostate cancer who have failed biochemically and 90 men treated for intermediate-risk prostate cancer who are biochemically free of disease. Patients were matched based on age, Gleason score, and number of intermediate risk factors. Each patient was treated with definitive proton therapy between 2006 and 2010 and each had a minimum of 2 years of follow-up. Contour accuracy was assessed by a team of radiation oncologists who were blind to each patient's name and treatment outcome, and accuracy was judged using a 4-point scale with 1 indicating acceptable contours and 4 indicating multiple major contouring errors thought to be undercontours of the prostate. The PrTV/PUV ratio was calculated and its relationship to the presence and severity of contouring errors was analyzed. The association of contouring errors to the presence of biochemical failure was also analyzed.

Results: The prostate PrTV/PUV ratio was significantly associated with contouring accuracy. As the median PrV/PUV ratio decreased from 1.42 to 0.92, the likelihood of a major contouring error was significantly higher (p=0.049). Eighty-three percent of patients with a PrTV/PUV ratio of less than 1 had a major contouring error. Biochemical failure was more common in patients with contouring errors (HR 1.5), but the association did not achieve statistical significance (p=0.35).

Conclusions: Before delivering radiation therapy treatment, quality assurance teams may be able to efficiently screen for and find contouring errors based on the PrTV/PUV ratio, which is often below 1 when major undercontouring of the prostate has occurred.

Comparison of Different Approaches to Robust Treatment Planning for IMPT

Presented by Joanna Gora, PhD (EBG MedAustron GmbH)

Creation of treatment plans robust against range and setup uncertainties is crucial for fractionated radiotherapy. For IMPT treatment planning it is of even more importance, as protons are extremely sensitive to density changes along their path. Conventional approach of dealing with such issues is

creation of the planning target volume (PTV). However, multiple studies showed that simple geometrical expansion of the clinical target volume (CTV) might not be sufficient for IMPT.

The purpose of this study was to test all currently available methods for IMPT treatment planning and evaluate which of them would be the most robust for skull base patients.

8 nominal treatment plans were created with the treatment planning system RayStation 4.7 for skull base cancer patients. The following planning strategies were used to generate the nominal plans: single field optimization (SFO), multiple field optimization (MFO), SFO with field specific margins (SFO-BSM), MFO with planning organ at risk volume concept (MFO-PRV) and finally 2 SFO and 2 MFO plans using different robust optimization strategies (for both CTV and OARs). Robust optimisation parameters were chosen to create plans robust against 3.5% density change and 2 or 3 mm shifts.

Evaluation was performed by recalculation of 12 perturbed dose scenarios for each nominal plan. Perturbations were introduced by scaling HUs by ± 3.5% combined with 3 mm shifts of the isocenter on the main axes. DVH parameters were compared.

As expected the magnitude of deviations of the perturbed dose was the highest for MFO. The decrease in D98% is up to 42Gy, where for other methods D98% is on average 2Gy higher. In terms of OARs sparing for MFO also the highest increase in D2% was reported (for chiasm up to 51Gy). SFO-BSM, MFO-PRV methods where a bit more robust in terms of CTV and OARs doses but not better than SFO alone. Robust optimization approaches on the other hand seemed to deal with dose perturbations the best. Not only decrease in D98% dose was the smallest but also sparing OARs was the least sensitive to perturbations. Additionally, it resulted in the lowest remaining volume at risk (RVR).

This study not only confirmed that simple PTV concept might not be sufficient for IMPT, but also showed how sophisticated robust optimisation techniques can significantly increase robustness of the plans, however it is up to the planner to choose adequate optimizer settings requiring thorough evaluation and understanding of the underlying algorithms.

Content Analysis of Proton Therapy–Related Twitter Traffic

Presented by Lauren Hintenlang, BS (Mayo Clinic)

Objectives: As one of the most popular microblogging platforms, Twitter provides a wide audience for the dissemination of information and encourages conversations about new ideas and current events. This study investigates the function of Twitter in radiotherapy by evaluating various facets of the Twitter traffic discussing proton therapy.

Methods: Using Rowfeeder (www.rowfeeder.com), a social media monitoring and analytic tool, data was collected for 1,100 consecutive tweets using the tag "proton therapy" from 30 July 2015 to 2 September 2015. The data was then sorted and analyzed based on the content of the tweet, its attitude towards proton therapy, the type of hyperlink it contained, and the type of cancer discussed. The country of origin and the number of potential impressions were also evaluated to provide a more complete perspective. These findings were then compared to a similar analysis conducted in 2013 (Miller, PTCOG, 2013).

Results: Approximately 44% of the tweets discussed commercial communications, 33% shared constructive information, 17% related personal experiences, about 4% were job related, roughly 1% were asking for information, and the remaining 1% were not translated from the original language or were classified as miscellaneous. Subjective categorizing of the posts found that a vast majority (84%) were neutral in regards to proton therapy, 15% were positive, and only 1% reflected negatively on proton therapy. Of the 20.5% of tweets discussing specific cancers, 38% involved pediatric cancer, 21% discussed cancers of the central nervous system (CNS), 19% pertained to prostate cancer, 15% cited cancers in other areas, and 7% mentioned cancers of the head and neck.

When compared to the results of the 2013 study, notable differences existed. Most significantly was the increase in commercial content from 16 to 43.5% and the decrease in negative attitudes from 7 to 1%. The number of potential impressions peaked at much higher numbers and the number of observed origin countries also doubled from 21 to 40.

Conclusion: Following global trends in social media, Twitter usage concerning proton radiotherapy has become more commercialized and more international in nature. The predominance of cancer specific Tweets on pediatric malignancies and the high frequency of links to fundraising sites suggests that social media applications remain an important tool for patient families and their social networks to communicate, advocate, and raise funds for treatment during proton therapy.

A Dosimetric Study of Prostate SBRT with Hydrogel Spacers Using Proton Pencil Beam Scanning Techniques

Presented by Nelly Ju, BS, RT(T), CMD (ProCure Proton Therapy Center)

Objectives: Intensity-modulated radiation therapy (IMRT) and volumetric-modulated arc therapy (VMAT) have demonstrated effectiveness for prostate cancer treatments. The potential advantage of proton therapy for prostate is to reduce rectal dose and the associated potential toxicity. For both photons and protons, patients typically are treated with 1.8-2 Gy per fraction to 76-80 Gy. Recent studies have suggested that stereotactic body radiotherapy (SBRT) is comparably effective for prostate cancer, while reducing the treatment time to 5 fractions. In this study, we perform a dosimetric comparison of the four-field SBRT versus two-field (bi-lateral) standard fractionation for prostate radiation therapy using proton pencil beam scanning (PBS) technique.

Materials and Methods: This study focuses on doses to the bladder, rectum, penile bulb, and femoral heads using a four-field (anterior oblique and bi-lateral) SBRT with PBS technique in single field uniform dose (SFUD) approach. Beam-on time per fraction is significantly higher due to the number of fields, however overall treatment time over the course of the treatment is significantly reduced. The patients chosen for this study had fiducial markers for image guidance, and hydrogel spacers placed between the rectum and the prostate. The latter are used to mitigate range uncertainties from the anterior oblique beams.

Results: We examined 5 cases for this pilot study. CTV coverage in the SBRT plan was maintained when compared to a standard 44-fraction PBS plan with 2 bi-lateral SFUD fields, in which the CTV V98%=100% and V100%>99% considering both the setup and range uncertainties.

Conclusions: The SBRT fractionation OAR constraints were evaluated against published guidelines. All maximum critical volumes above threshold doses could be met. Our results suggest that PBS SBRT for prostate cancer with hydrogel spacers is feasible.

Commissioning of Spot Measurement Equipment in a Light Ion Beam Therapy Facility: The MedAustron Experience.

Presented by V. Letellier, MSc (EBG MedAustron GmbH)

The purpose of this work is to report on the MedAustron experience and guide medical physicists in the implementation of spot measurement equipment as a pre-requisite to acceptance testing, commissioning and QA checks of light-ion beam therapy (LIBT) delivery systems. Emphasis is given to IBA Lynx PT, a 2D detector based on a scintillator and a 0.5 mm resolution CCD camera.

EBT3 radiochromic films were used as reference detector to commission the Lynx regarding spot position, spot size and homogeneity. EBT3 films were scanned with EPSON flat scanner providing 0.17mm resolution (150DPI) and 0.5% homogeneity after irradiation with a dose of 2Gy. Scintillator performances (linearity in dose, repeatability, homogeneity), optics capabilities (geometrical distortion, video, landmarks alignment, saturation, iris hysteresis) and positioning uncertainties were evaluated. A Lynx holder was designed and assembled in-house to position the Lynx on its 4 different faces with a higher level of accuracy and reproducible on the treatment couch of the irradiation room. Positioning and position validation could be also based on laser tracker targets. As no analysis tools for pencil beam scanning (PBS) were provided, a Python software was developed to extract automatically the spot and 2D field properties (size, position, skewness, ellipticity, penumbra) from Lynx videos and images. During commissioning, standard operating procedures were set up to optimize the usage and performances.

Inside its 10 x 10cm centered part the Lynx homogeneity was smaller than 3% and the differences between image and video acquisitions were below 0.2mm for spot size and position measurements. Using the room lasers, the absolute positioning uncertainties were respectively about 0.5mm, which can be reduced to 0.2mm using laser tracker. Landmark alignment showed geometrical calibration variations of about 0.5mm depending on the orientation of the Lynx on the couch. A comparison of Lynx vs. EBT3 films showed agreement of measured spot sizes and their position within 0.2mm).

In conclusion, the measurement equipment serves the needs of a newly setup LIBT facility. The equipment commissioning phase guaranteed a smooth implementation of the equipment for beam delivery commissioning and daily quality assurance.

Dosimetric Evaluation of Three Chest Wall Patients Treated with a Compact Proton Pencil Beam Gantry Utilizing a Multi-Isocenter, Linear Gradient-Matching Planning Technique and Daily CBCT and Stereoscopic Imaging.

Presented by Matthew Maynard, PhD (Willis-Knighton Cancer Center)

Purpose: To verify the ability of a compact proton pencil beam gantry with limited field size (20cm x 24cm) and image guidance capability to successfully treat patients with large-area targets such as left and right chest wall.

Methods: Our center employs a multi-isocenter, linear gradient-matching technique during treatment planning of proton chest wall patients. Each fraction includes a setup CBCT, automatic couch shifts to subsequent isocenters, and stereoscopic imaging to verify couch shifts. Daily couch shifts between treatment field isocenters were obtained for each fraction from the record and verify system. Copies of the initial treatment plan were made for each fraction and the field isocenter coordinates for each plan were

adjusted to reflect daily couch shifts. Doses were re-calculated for each fraction, summed, and compared against the initial plan.

Results: Dose differences to the planning volume, heart and ipsilateral lung were evaluated. Percentage of the target volume receiving the prescription dose (planned vs. isocenter-shifted) for the three cases: 89.0% vs. 94.6%, 95% vs. 96%, and 90% vs. 92%. Percent volume of the ipsilateral lung receiving 20Gy (planned vs. isocenter-shifted) for the three cases: 18.5% vs. 21%, 6.1% vs. 5.7%, and 12.6% vs. 12.8%. Hot spots (% of prescription dose) within the ipsilateral lung volume (planned vs. isocenter-shifted) for the three cases: 5.1% vs. 6.4%, 4.9% vs. 12.6%, and 7.0% vs. 8.2%. Hot spots (% of prescription dose) within the target volume (planned vs. isocenter-shifted) for the three cases: 6.6% vs. 9.3%, 7.3% vs. 14.4%, and 7.1% vs. 8.3%. Mean heart dose differences were negligible in all three cases.

Conclusions: Observed dose differences to lung and heart tissues due to daily setup variations remained acceptably low while maintaining sufficient dose coverage to the target volume. This study demonstrates the ability of a compact proton pencil beam gantry with limited treatment field size to utilize multiple isocenters, a linear gradient-matching planning technique, and daily CBCT and stereoscopic imaging to successfully treat a chest wall patient. These techniques could also be applied to other large-area targets such as whole pelvis with para-aortic lymph nodes.

Postoperative Proton Therapy for Pancreatic Cancer Patients Enrolled on the Proton Collaborative Group (PCG) Registry.

Presented by R. Charles Nichols Jr., MD (University of Florida)

Background: The PCG registry is a multicenter registry for patients receiving proton therapy for various malignancies. The current abstract reviews the outcomes for patients receiving postoperative proton therapy for resected pancreatic cancer.

Methods/Materials: From 2/2013 to 6/2015 12 patients with resected pancreatic adenocarcinoma received postoperative proton therapy. The current study reviews the pretreatment characteristics and outcomes of these patients.

Results: Median age=72 years (range, 52 to 79); 8 Males, 4 Females; T Stage: T2=3, T3=8, T4=1; N Stage: N1=10, N0=0; Margin Status: Close=5, Positive=3, Negative=4; Surgical approach: open=10, laparoscopic=2; Operations performed: standard pancreaticoduodenectomy=7, pylorus sparing pancreaticoduodenectomy=4, total pancreatectomy=1; Median lymph nodes taken=19.50 (range, 11 to 72); Median lymph nodes positive=2 (range, 0 to 7); PNI positive=9, PNI unknown=3; LVI positive=6, LVI negative=3, LVI unknown=3; Median tumor size=3cm (range, 2.2 to 6.2); Median dose delivered=50.51Gy(RBE) (range, 27.88 to 54.00); Median treatment duration=38 calendar days (range, 25 to 48).

One patient died during treatment. Only one patient's treatment was protracted by more than 5 days. Median available follow up is 0.9 year (range, 0.07 to 1.7 years); 1 year survival was 54%.

Conclusion: Postoperative proton therapy after pancreatectomy was well tolerated without significant toxicity or treatment interruption.

Two PBS Treatment Planning Techniques for Breast Patients with Tissue Expanders Containing High Density Metallic Filling Ports.

Presented by Mark Pankuch, PhD, DABR (Northwestern Medicine Chicago Proton Center)

Objectives: To develop treatment planning methods using Intensity Modulated Proton Therapy (IMPT) to produce treatment plans that deliver the prescribed doses to the target tissues in the presence of a breast tissue expander containing a high density metallic filling port. Due to the challenges in the accuracy of calculating proton scattering and proton path lengths through a high density filling port, each method includes the elimination of all proton spots that have a potential to pass through the port. The use of such methods would eliminate the added complexity and inaccuracies in calculations of particles passing through the metallic port.

Methods: Two proton institutions have developed two planning techniques that are constrained in the planning process to prohibit any spots downstream of the metallic filling port. One method uses two PBS beams that omit all spots downstream of the defined metallic port. The two field's spot weights are determined using a multi field iterative optimization to deliver a cumulative uniform dose to the target regions around the port. Gantry angles are chosen to allow the target shadowed by any one field to be supplemented by doses delivered by the complementary field. A second method separates the target regions around the port into two, non-overlapping structures. Two treatment fields are used with each individual field optimized to deliver the full dose to only one of the two split target sections. Gantry angle selection and delineation of the target splitting position are dependent of the patient's specific anatomy.

Results: Using the methods described, treatment plans have been developed that demonstrate appropriate target coverage in regions containing a metallic filling port. To minimize the sensitivities to set-up errors and range uncertainty, regions superior and inferior to the metallic filling port were optimized such that each of the two beams delivered half of the prescribed dose to these specific areas. This segregation of optimization areas was used to increase overall plan robustness.

Conclusions: Two IMPT planning methods that use two complementary beam angles to treat breast targets around a metal filling port have been developed. Sensitivities to set-up error can be reduced by separating the target areas into distinct portions dependent on their location relative to the metallic filling port.

Pencil Beam Scanning for Bilateral Breast Treatments

Presented by Mosa Pasha, RT(T), CMD (Princeton ProCure NJ)

Objective: Bilateral breast radiation treatment can present both treatment time and dosimetric challenges for patients with nodal involvement. We sought to demonstrate the characteristics of a bilateral breast pencil beam scanning (PBS) plan using a single-field, mono-isocentric technique in a patient with bilateral breast cancer and lymphatic involvement.

Methods: Bilateral breast treatment planning was performed on a female patient with synchronous stage I and stage II invasive ductal carcinomas treated with breast conserving therapy. The prescription dose to the bilateral breasts and unilateral lymph nodes was 46 CGE in 2 CGE fractions. We created a single, en face AP field using an IBA gantry. A 7.5 cm range shifter and a 30 x 40 snout were used to generate the plan utilizing RayStation treatment planning system. The minimum air gap was 5 cm. Couch was set to

270 degrees to allow the larger aspect of the 30 x 40 snout to cover the target. The CTV volume included the entire breast, chest wall, unilateral axilla and lymph nodes. The PTV expansion for the whole volume was 7mm (4mm post above lung), excluding ribs and intercostal muscles.

Results: PTV V95 was 99.6%; total lung V20 was 6.6%; mean heart dose was 0.03 Gy; max dose to 0.5cc of skin was 46.79 Gy. A total of 34 energy layers with ~8300 MU were used to cover a PTV with a 2100 cc volume. Maximum point dose to the PTV was 105%. Plan was robust for variations in both range (3.5%) and setup (5 mm). Additionally, dose homogeneity and delivery times were improved due to the larger snout size, requiring no match lines with a single isocenter approach.

Conclusion: While this is a single case study, it does suggest that PBS can successfully and efficiently treat patients with bilateral breast cancer. Compared to IMRT and 3D tangent photon plans, all OAR doses are lower, notably the heart and lungs.

Intensity Modulated Proton Therapy Planning for Low-Risk Prostate Cancer Based on Proton Collaborative Group (PCG)-GU002-10 (NCT01230866) Protocol

Presented by Suresh Rana, MS (McLaren Proton Therapy Center)

Purpose: The purpose of this study is to investigate whether proton collaborative group (PCG)-GU002-10 (NCT01230866) protocol's dosimetric criteria can be applied for low-risk prostate cancer treatment plans generated by intensity modulated proton therapy (IMPT) technique.

Methods: A total of ten low-risk prostate cancer cases were included in this retrospective study. Clinical target volume (CTV) included prostate only, whereas planning target volume (PTV) was expanded from the CTV (margin: 2 mm to the posterior and 3 mm elsewhere). Optimization target volume (OTV) was generated from the CTV (margin: 2 mm to the posterior, 5 mm left and right, and 3 mm elsewhere). Scanning target volume (STV) was generated from the OTV (margin: 7 mm). For each case, two IMPT plans were generated using single field optimization (SFO) and multi-field optimization (MFO) techniques in Eclipse treatment planning system (version 11) for treatment to be delivered with 1.8 Gy(RBE) per fraction for a total prescription dose (PD) of 79.2 Gy(RBE). Each plan was generated using two parallel opposed lateral fields. Both sets of plans (SFO-IMPT and MFO-IMPT) were optimized using identical dose constraints with an objective of meeting the protocol criteria. Treatment plans were then normalized such that at least 95% of the OTV received the PD. (i.e., 79.2 Gy(RBE))

Results: All ten cases produced PTV D99.5% > 75.24 Gy(RBE) (SFO-IMPT: 77.17±0.98 Gy(RBE); MFO-IMPT: 77.21±1.02 Gy(RBE)). The CTV D99% was 100.85±0.74 % of PD in SFO-IMPT plans and 100.81±0.70 % of PD in MFO-IMPT plans. For the rectum, V50 was less than < 35% (SFO-IMPT: 10.11±6.12 %; MFO-IMPT: 10.30±6.20 %) and V70 was less than 10% (SFO-IMPT: 3.82±2.76 %; MFO-IMPT: 3.83±2.64 %). For the bladder, V80 was less than 8 cc (SFO-IMPT: 2.85±3.04 cc; MFO-IMPT: 2.75±2.94 cc). For the femoral heads, V45 was 0 in all ten cases.

Conclusion: Based on the results from this study, both the SFO-IMPT and MFO-IMPT plans met the dosimetric criteria of PCG-GU002-10 (NCT01230866) protocol without any deviation. It is feasible to apply dosimetric criteria of PCG-GU002-10 (NCT01230866) protocol for low-risk prostate cancer plans generated by IMPT techniques.

Development of a Metric for Knowledge-Based Robust Planning for Head and Neck

Presented by Jackson Renegar, MS, DABR (Provision Proton Therapy Center)

Proton therapy can provide clinical advantages due to its ability to deliver highly conformal dose distributions with minimal dose to surrounding tissues. However, this can also make proton treatments especially susceptible to patient setup or treatment delivery uncertainties. To address these uncertainties, at the Provision Proton Therapy Center, each plan goes through a "Robust Analysis" where uncertainties are simulated in the Treatment Planning System, yielding perturbed doses, which are evaluated against clinical goals to determine plan acceptability.

Following treatment start, patients judged to have significant uncertainty are scheduled for periodic "QA CT" scans. The results of these scans determine the need for adaptive planning. Based on our recent data, 80% of non-prostate patients received QA CT scans, and 30% had adaptive plans. Without cone-beam CT in the IBA treatment rooms, this requires setup of the patient in the treatment position in the CT simulator. It is therefore necessary to balance the desire for frequent QA CT's with the need to minimize additional dose to the patient, as well as the demands of a busy CT simulator schedule.

Focusing on bilateral head and neck patients, data was compiled to correlate the results of the initial robust analysis of the plan with subsequent results of QA CT's. The goal was to develop a metric for plan robustness, which could be applied to future cases to quantify the uncertainty of the plan, and possibly help determine an appropriate frequency for QA CT's.

DVH data was exported for the nominal treatment plan, six 4 mm isocenter shifts, positive and negative CT density shifts, and positive and negative roll and rotation. Because perturbing the treatment plan in this manner tends to create a shoulder to the target DVH curve, the standard deviations of D98 and D95 of the above listed 13 DVH curves were calculated for each sample patient. The reduction in D98 and D95 on subsequent QA CT's was plotted against the standard deviations from the robust evaluation.

The results show a rough, positive correlation between robust analysis results on a given treatment plan, and how well the plan holds up on QA CT scans. This model needs further development before it can be applied to determining relative necessity for QA scans, however will likely be valuable as a type of knowledge based planning metric for comparing robustness of a newly created plan against the robustness of previously created plans of the same type.

A Comparison of Two PBS Treatment Planning Techniques for Locally Advanced Breast Cancer: PTV vs. Robust CTV

Presented by Stacey Schmidt, CMD (Northwestern Medicine Chicago Proton Center)

Background: Seven, left-sided locally advanced breast cancer patients were planned with two separate treatment planning techniques using pencil beam scanning (PBS) proton delivery. The study's purpose is to compare target coverage and doses to critical organs at risk (OARs).

Method and Materials: The first treatment planning technique consisted of two PBS beams with gantry angle separations averaging 0 degrees apart. For these plans, a planning volume was created on the average gantry angle and shifted in the distal direction of the beam path to account for set-up and range uncertainties. This planning volume was then intersected with the clinical target volume (CTV) minus skin

structure and was used as a method to attempt to achieve robust optimization. The second treatment planning technique consisted of a single, enface beam, which was optimized to the CTV minus skin structure. In the second technique, robustness was achieved by using the treatment planning system's built in robust planning module. Robustness optimization criteria for the set-up uncertainties in the x,y and z directions of 5 mm in magnitude were used. Range uncertainty was not included in the robust optimization, but was included in the robustness evaluation.

Results: All plans were evaluated for robustness by looking at 27 different scenarios using +/- 3.5% for range uncertainties, and a vector of 7 mm. A paired t-test was utilized to assess statistical significance between the two planning types. CTV coverage was comparable between the two planning methods. Doses to heart (V(5Gy(RBE)) , V(20Gy(RBE)) , D(1cc), ipsilateral lung V(5Gy(RBE)) and mean esophagus dose were statistically equivalent between the two planning methods (p>>0.05). The average V(20Gy(RBE)) of the ipsilateral lung on the single field plan was 14.3%, +/- 2.0%. This was significantly better than the two field plan with an average ipsilateral V(20Gy(RBE)) of 22.1%, +/- 6.9% (p=0.03).

Conclusion: In this seven patient study, the single field technique using robust optimization methods was able to achieve comparable target coverage to a two field method using beam-specific optimization structures. Except for an improved V(20Gy(RBE)) in the single field plan, there were no statistically significant differences to doses to OARs.

High Resolution, Fast Proton Range Verification with Multi-Layer Ion Chamber and Dynamic Passive Degrader Tandem Assembly

Presented by J. Stoker, PhD, DABR (Mayo Clinic)

Introduction: Determining the range in water is an essential component of proton beam quality assurance. This range is initially determined with high precision during beam commissioning by water tank relative depth dose (RDD) scans. Typical proton treatment systems deliver of order 100 unique energies, so range commissioning can consume up to a week of beam time. This work details a method to reduce the time required for periodic range validation to under 2 hours.

Method: We employed a multi-layer ion chamber (MLIC) (Hitachi, Ltd. Tokyo, Japan) assembly, with 104 individual ion chambers placed at 4-mm water equivalent thickness (WET) intervals to collect RDD data. Upstream of the MLIC was a dynamic passive-degrader assembly (DPDA), which housed retractable degraders of 3.2, 1.6, 0.8, 0.4, and 0.2 mm WET. The MLIC and DPDA were triggered by a synchrotron sextuple magnet, which sends a pulse with each beam extraction. 20 unique degrader combinations were programmed to shift the DPDA WET by 3.8 mm in 0.2-mm steps, then repeated for each of 97 energies. 80 MU (4 MU per extraction) were delivered for each energy to obtain 0.2-mm resolution RDD scans. The delivery control files were automated to deliver 20-energy batches, then paused to allow for an intermediate save of the data to disk. In-house software facilitated and automated distal 80% range (R80) extraction.

Results: Each 4-MU extraction requires approximately 2.5 seconds to deliver. Including pauses, the 97-energy dataset was collected in approximately 90 minutes. Measured R80s for the set deviated on average from commissioned values by 0.1 ± 0.3 mm (range -0.5:0.7 mm). Range variation among subsequent acquisitions of MLIC data collected over a 9 month period was an order of magnitude smaller: 0.04 ± 0.09 mm (range 0.0:0.4 mm).

Conclusions: Interfacing hardware and software with the beam delivery system allows for rapid acquisition of RDD scans. The 90 minute acquisition time is much smaller than the week-long effort required for water tank scans, and makes periodic verification of the full spectrum of proton energies tractable. Direct comparison to water tank measurements yielded deviations greater than our acceptance testing tolerance of 0.5 mm. Nevertheless, the high reproducibility of MLIC data makes the device and approach valuable for periodic constancy verification.

Multiple-Coulomb-Scatter Based Proton Radiography With Pencil Beam

Presented by Rachel Windmueller (Rhodes College) and Weiguang Yao, PhD (St Jude Children's Research Hospital)

Purpose: Multiple Coulomb Scatter (MCS) continues to provide a challenge for proton radiography in improving resolution and contrast. We propose to use the statistics of the proton fluence to form proton radiographs.

Methods: The MCS fluence at a detector plane can be well approximated as a Gaussian distribution, particularly in the proton radiography scenario. The standard deviation (SD) of the distribution increases as the water equivalent thickness along the pencil beam path increases. Thus, the image of the SD displays unique anatomic information of the patient body and can be used for patient positioning.

Prior to obtaining the radiograph with our proton pencil beam scanning facility, a TOPAS Monte Carlo code was developed to simulate the radiograph of a patient's head. This particular scan utilized 40,000 individual proton pencil beams in 1 mm separation at energy of 221.28 MeV, with a total dosage of 0.5 mGy. The fluence from each pencil beam was recorded and the SD was calculated. The calculation of all the SDs took approximately 40 seconds on an Intel(R) Xeon(R) E5-2680 v3 at 2.50GHz. The acquisition of the fluence from our proton facility was conducted by a Lynx(R) 2D scintillator detector with a CCTV that provides a read out of the proton exposure. A radiograph was also made with EBT3 films. The spots were positioned with a 2.76 mm separation and covered 20 cm x 25 cm. The phantom used in this radiograph was a pediatric head phantom.

Results: While the results from the proton beam are still underway, the Monte Carlo simulation has produced a high quality radiograph where the patient's anatomic structures are recognizable. On the contrary, the radiograph created by the fluence itself is extremely blurry.

Conclusion: Our proton radiography based on the statistical property of MCS results in a high quality image of the patient's anatomic structures. This study moves forward in the search for a reliable imaging tool for protons and to use in proton therapy. These radiographs are a solid base for a further investigation towards a dependable imaging modality in proton radiology.

A Simplified Analytical Random Walk Model for Proton Dose Calculation

Presented by Weiguang Yao, PhD (St Jude Children's Research Hospital)

Purpose: To balance the accuracy with the computation time, we propose an analytical random walk model for proton dose calculation in a laterally homogeneous medium.

Method and Materials: A formula for the spatial fluence distribution of primary protons was derived. The variance of the spatial distribution is in the form of a distance-squared law of the angular distribution. To improve the accuracy of dose calculation in the Bragg peak region, the energy spectrum of the protons was used. The accuracy was validated against TOPAS Monte Carlo simulation in water phantoms with either an air gap or a slab of bone inserted. We further applied the algorithm to patients' cases in the highly heterogeneous head and pelvis sites and used a gamma test to show the reasonable accuracy of the algorithm in these sites. Particularly, we examined the accuracy of our algorithm in a small size pencil beam (micro-beam), and in the dependence upon depth of the heterogeneous slab in water.

Results: For water phantoms, the dose calculated by our algorithm excellently matched that predicted from MC simulations, with a slight difference of approximately 1% between the ranges at energies 165 MeV and 195 MeV. For a 2 mm pencil beam traversing through water phantoms embedded with various thicknesses of air gaps (0 cm, 10 cm and 40 cm), the relative dose difference was within 1%. For the patient cases, the 2D gamma test (3%/3mm/10%) pass-rates for our algorithm against MC simulations were 95.2% in head and 96.0% in pelvis. Finally, from the depth dose curve and lateral profiles, our algorithm excellently captured (within 1%) the dose dependence on depth of a slab of bone embedded in water medium at 1 cm and 11 cm from the water surface. Our algorithm is fast for clinical use. For a 5×5 cm2 proton beam of 150 MeV in water with the voxel resolution 1×1×1 mm2, the algorithm took less than 2 minutes in a single CPU (Intel(R) Xeon(R) CPU E5-2680 v3 @ 2.50GHz).

Conclusion: The algorithm accurately reflects the dose dependence on the depth of the bone and can deal with small-field dosimetry. The high accuracy of our algorithm in media with large air gap indicates its application in treatment plans with range shifters.

Acknowledgements

We are pleased to acknowledge the sponsors of the social events and meals associated with this conference.

HITACHI
Inspire the Next

Diamond Sponsor
Gala at Bass Pro Shops at the Memphis Pyramid

MEVION
medi | systems

Platinum Sponsor, Dinner at the National Civil Rights Museum

iba

Gold Sponsor, Lunch at the Domino's Event Center on Tuesday

RaySearch Laboratories

Gold Sponsor, Memphis Blues at the Beale Street Landing (hors d'oeuvres)

VARIAN
medical systems
Particle Therapy

Gold Sponsor, Lunch at the Domino's Event Center on Monday

Orfit, Protom, and .decimal

Silver Sponsors

St. Jude Maps

Marlo Thomas Center for Global Education and Collaboration

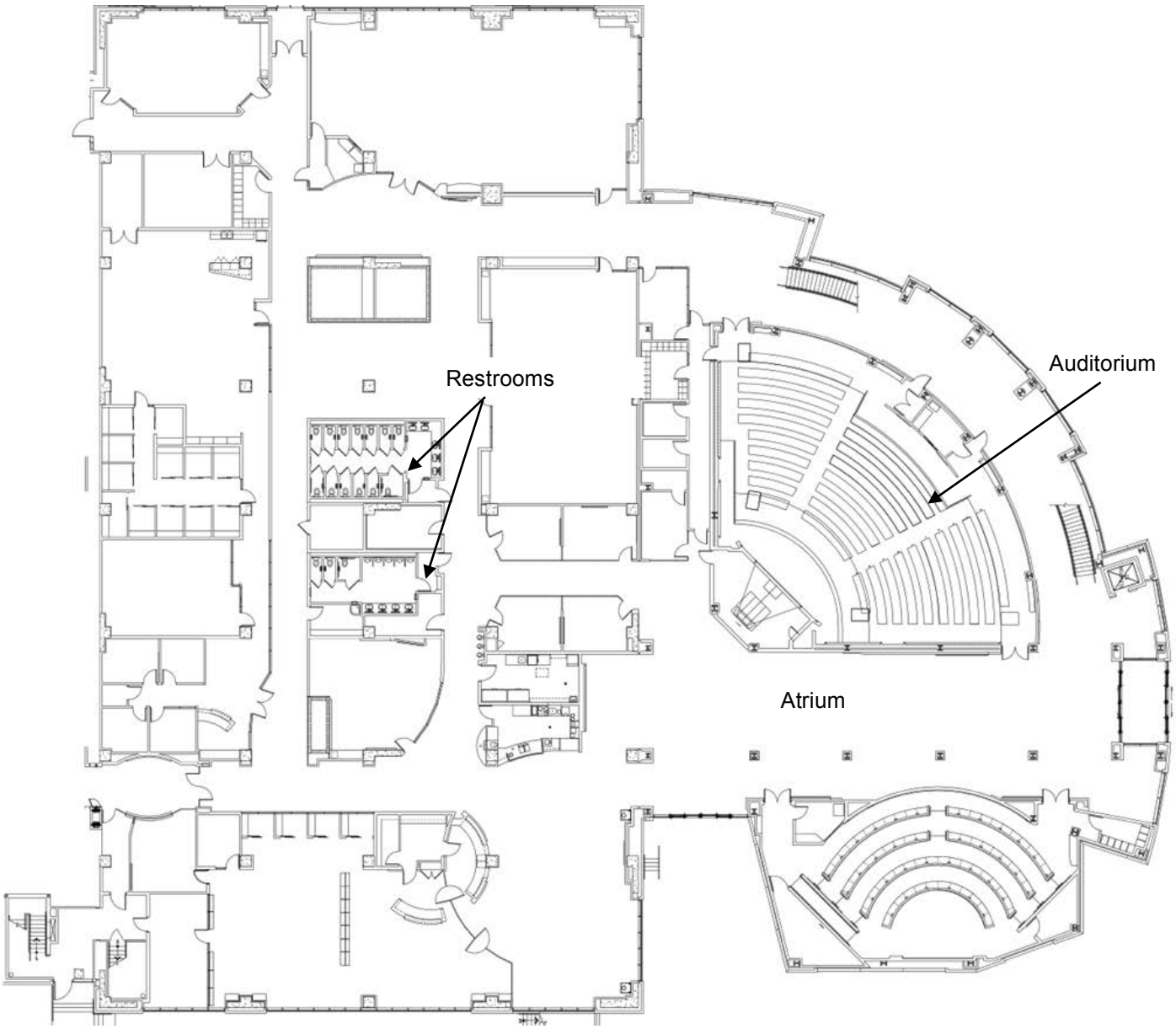

Campus Map

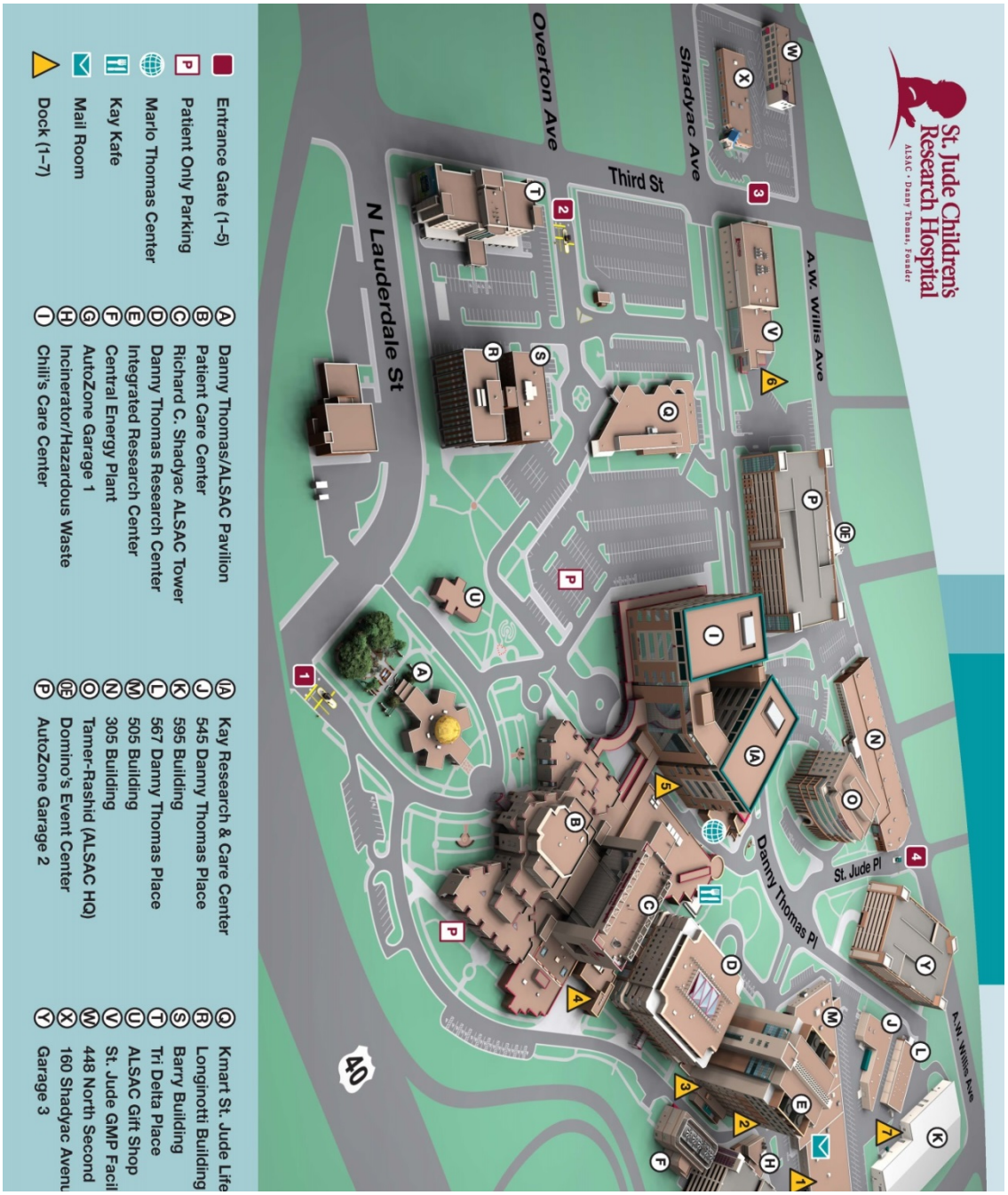
St. Jude Children's Research Hospital
ALSAC • Danny Thomas, Founder
A.W. Willis Ave
Shadyac Ave
Third St
Overton Ave
N Lauderdale St
St. Jude Pl
Danny Thomas Pl
40
Entrance Gate (1–5)
Patient Only Parking
Marlo Thomas Center
Kay Kafe
Mail Room
Dock (1–7)
A Danny Thomas/ALSAC Pavilion
B Patient Care Center
C Richard C. Shadyac ALSAC Tower
D Danny Thomas Research Center
E Integrated Research Center
F Central Energy Plant
G AutoZone Garage 1
H Incinerator/Hazardous Waste
I Chili's Care Center
IA Kay Research & Care Center
J 545 Danny Thomas Place
K 595 Building
L 567 Danny Thomas Place
M 505 Building
N 305 Building
O Tamer-Rashid (ALSAC HQ)
PE Domino's Event Center
P AutoZone Garage 2
Q Kmart St. Jude Life
R Longinotti Building
S Barry Building
T Tri Delta Place
U ALSAC Gift Shop
V St. Jude GMP Facil
W 448 North Second
X 160 Shadyac Avenu
Y Garage 3